EFFECT OF GAP DISTANCE ON THE MECHANICAL PROPERTIES AND CROSS-SECTIONAL CHARACTERISTICS OF THE MIG-MAG BUTT WELDS

A THESIS SUBMITTED TO
THE GRADUATE SCHOOL OF NATURAL AND APPLIED SCIENCES
OF
THE MIDDLE EAST TECHNICAL UNIVERSITY

BY

İLKER KAŞIKÇI

IN PARTIAL FULFILLMENT OF THE REQUIREMENTS FOR THE DEGREE OF
MASTER OF SCIENCE
IN
THE DEPARTMENT OF METALLURGICAL AND MATERIALS ENGINEERING

JULY 2003

Approval of the Graduate School of Natural and Applied Sciences.

Prof. Dr. Canan ÖZGEN
Director

I certify that this thesis satisfies all the requirements as a thesis for the degree of Master of Science.

Prof. Dr. Bilgehan ÖGEL
Head of Department

We certify that we have read this thesis and in our opinion it is fully adequate, in scope and quality, as a thesis for the degree of Master of Science in Metallurgical and Materials Engineering.

Prof. Dr. Alpay ANKARA
Supervisor

Examining Committee Members:

Prof. Dr. Alpay ANKARA

Assoc. Prof. Dr. Rıza GÜRBÜZ

Assoc. Prof. Dr. Ali KALKANLI

Assoc. Prof. Dr. Hakan GÜR

Assist. Prof. Dr. Kazım TUR

ABSTRACT

EFFECT OF GAP DISTANCE ON THE MECHANICAL PROPERTIES AND CROSS-SECTIONAL CHARACTERISTICS OF THE MIG-MAG BUTT WELDS

Kaşıkçı, İlker

M.S, Department of Metallurgical and Materials Engineering

Supervisor : Prof. Dr. Alpay Ankara

July 2003, 64 pages

This study was undertaken with the objective of determining the effect of gap distance on the weld bead geometry and the mechanical properties of the weldments. Low-alloyed and low carbon steel plates were welded under different conditions where each weldment had different gap distance and weld bead grooves. The influences of welding parameters namely, welding speed, current and voltage on the weld bead were examined in terms of weld bead penetration and heat affected zone and weld metal zone hardness variations.

Key words : MIG-MAG welding, butt welds, weld bead.

ÖZ

METAL-KORUYUCU GAZ İLE YAPILAN ALIN KAYNAKLARINDA, PLAKALAR ARASI MESAFENİN, KAYNAK KESİT VE MEKANİK ÖZELLİKLERİNE ETKİSİ

Kaşıkçı, İlker
Yüksek Lisans, Metalurji ve Malzeme Mühendisliği Bölümü
Tez Yöneticisi : Prof. Dr. Alpay Ankara

Temmuz 2003, 64 sayfa

Bu çalışma, plakalar arası mesafenin, kaynak dikişi geometrisi ve mekanik özellikleri üzerine etkisini belirlemek amacıyla gerçekleştirilmiştir. Farklı plakalar arası mesafe ve kaynak ağzı hazırlığı yapılmış olan düşük karbonlu ve düşük alaşımlı çelik plakalar, çeşitli kaynak koşullarında kaynaklanmıştır. Kaynak parametrelerinin, sırasıyla, kaynak hızı, akımı ve voltajın, kaynak dikişi üzerindeki etkileri, kaynak nüfuziyeti, ısıdan etkilenmiş bölge ve kaynak metali bölgelerindeki sertlik değişimleri yardımıyla incelenmiştir.

Anahtar Kelimeler : Metal-koruyucu gaz kaynağı, alın kaynağı, kaynak dikişi

ACKNOWLEDGMENTS

I wish to express my sincere gratitude to Prof.Dr.Alpay Ankara for his valuable supervision, guidance, encouragement and constant support in preparing this thesis during which many of the obstacles would be hard to overcome without his helps.

I express my sincere appreciation to Mr. Caner Batıgün and Welding Technology Center staff for their patient supervision, guidance and insight throughout the research.

I would like to thank especially to my family.

TABLE OF CONTENTS

ABSTRACT iii
ÖZ iv
ACKNOWLEDGMENTS v
TABLE OF CONTENTS vi
LIST OF TABLES viii
LIST OF FIGURES ix
CHAPTER
1. INTRODUCTION 1
2. LITERATURE SURVEY 3
2.1 Gas Metal Arc Welding 3
2.2 Fundamentals of the Process 4
2.3 Process Variables 6
2.3.1 Welding Current 6
2.3.2 Polarity 8
2.3.3 Arc Voltage (Arc Length) 9
2.3.4 Travel Speed 11
2.3.5 Electrode Extension 11
2.3.6 Electrode Orientation 12
2.3.7 Electrode Size 14
2.3.8 Shielding Gases 14
2.3.9 Equipment 16
2.3.9.1 Electrode Feed Unit 17
2.3.10 Metal Transfer Mechanisms 17
2.3.10.1 Short Circuiting Transfer 17
2.3.10.2 Globular Transfer 19
2.3.10.3 Spray Transfer 21

3. EXPERIMENTAL 24
3.1 Materials Used 24
3.1.1 Base Metals 24
3.1.2 Filler Metal 25
3.1.3 Shielding Gas 26
3.2 Experimental Set-up 26
3.3 Experimental Procedure 29
3.3.1 Sample preparation 29
3.3.2 Visual Inspection of the Specimens 30
3.3.3 Metallographic Specimen Preparation 31
3.3.4 Hardness Test 31
3.3.5 Bead Penetration Measurement 33
3.3.6 Tensile Test 33
3.3.7 Dilution Analysis 35
4. RESULTS AND DISCUSSION 36
4.1 Presentation of Results 36
4.2 Effect of heat input rate on hardness 39
4.3 Effect of gap distance on hardness 40
4.4 Effect of bevel height on hardness 50
4.5 Effect of gap distance, bevel height and heat input on penetration 52
4.6 Dilution analysis results 55
4.7 Tensile test results 59
5. CONCLUSIONS 61
REFERENCES 63

LIST OF TABLES

TABLE

3.1	Chemical compositions of S235 and 31CrV3	25
3.2	Chemical composition of G3Si1	26
3.3	Motor calibration values	29
3.4	Weld joint dimensions of S235 and 31CrV3	30
3.5	Denomination and symbols of the tensile test specimen	34
4.1 (a)	Tabulated values of the process variables used in the experiments for S235	36
4.1 (b)	Tabulated values of the process variables used in the experiments for 31CrV3	38
4.2	The selected specimens with corresponding process variables	39
4.3	Hardness values (H_v) at constant gap distance over bevel height ratio	39
4.4	Hardness values (H_v) at 2.42 kj/cm	41
4.5	Hardness values (H_v) at 3.18 kj/cm	45
4.6	Hardness values (H_v) at constant gap distance	50
4.7	Bead penetration and the corresponding process variables	53
4.8	Chemical compositions of 31CrV3 on the base metal and specimens 50, 51,52	55
4.9	Hardness values (H_v) of 31 CrV3 at 3.55 kj/cm	55
4.10	Tensile test results	59
4.11	Mechanical properties of the weld metal and S235	60

LIST OF FIGURES

FIGURE

2.1	Gas Metal Arc Welding Process	5
2.2	Typical welding currents versus wire feed speeds for carbon steel electrodes	7
2.3	Gas metal arc welding terminology	10
2.4	Effect of electrode position and welding technique	13
2.5	Gas-metal arc welds with argon and 75% He-25% Ar	15
2.6	Schematic representation of short-circuiting metal transfer	19
2.7	Non axial globular transfer	20
2.8	Variation in volume and transfer rate of drops with welding current (Steel electrode)	22
3.1 (a)	Quicky motor	27
3.1 (b)	Shielding gas and its regulator	27
3.1 (c)	Welding machine	28
3.2	Single V-groove butt joint preparations	29
3.3 (a)	Corresponding regions of the macrosection of the specimens	32
3.3 (b)	Indentation profile on the macrosection of the specimens	32
3.4	A schematic diagram for bead penetration, width and height	33
3.5	Tensile Test Specimen	34
4.1	Effect of heat input rate on hardness (at constant gap distance over bevel height ratio (1/3))	40
4.2	Effect of gap distance on hardness (at constant heat input rate, (2.42 kj/cm) and bevel height (3 mm))	41

4.3 (a) Visual appearance of the specimen 40 (cap) 42
4.3 (b) Visual appearance of the specimen 40 (root) 42
4.3 (c) Macro-photograph of the specimen 40 42
4.4 (a) Visual appearance of the specimen 44 (cap) 43
4.4 (b) Visual appearance of the specimen 44 (root) 43
4.4 (c) Macro-photograph of the specimen 44 43
4.5(a) Visual appearance of the specimen 48 (cap) 44
4.5(b) Visual appearance of the specimen 48 (root) 44
4.5(c) Macro-photograph of the specimen 48 44
4.6 Effect of gap distance on hardness (at constant heat input rate, (3.18 kj/cm) and bevel height (3 mm)) 45
4.7 (a) Visual appearance of the specimen 8 (cap) 46
4.7 (b) Visual appearance of the specimen 8 (root) 46
4.7 (c) Macro-photograph of the specimen 8 46
4.8 (a) Visual appearance of the specimen 12 (cap) 47
4.8 (b) Visual appearance of the specimen 12 (root) 47
4.8 (c) Macro-photograph of the specimen 12 47
4.9 (a) Visual appearance of the specimen 16 (cap) 48
4.9 (b) Visual appearance of the specimen 16 (root) 48
4.9 (c) Macro-photograph of the specimen 16 48
4.10 Effect of bevel height on hardness (at constant heat input rate, 3.55 kj/cm and gap distance, 1 mm) 50
4.11 Macro-photograph of the specimen 30 51
4.12 Macro-photograph of the specimen 31 51
4.13 Macro-photograph of the specimen 32 51
4.14 Comparison of measured and calculated bead penetration 53
4.15 Effect of arc oscillation on microstructure 54
4.16 Effect of gap distance on hardness, at constant heat input rate 56
4.17 Macro-photograph of the specimen 50 57
4.18 Macro-photograph of the specimen 51 57
4.19 Macro-photograph of the specimen 52 57

CHAPTER 1

INTRODUCTION

Welding is one of the most important and versatile means of fabrication available to industry. Welding is used to join hundreds of different commercial alloys in many different shapes. Actually, many products could not even be made without the use of welding, for example, guided missiles, nuclear power plants, jet aircraft, pressure vessels, chemical processing equipment, transportation vehicle and literally thousands of others.

Many of the problems that are inherent to welding can be avoided by proper consideration of the particular characteristics and requirements of the process. Proper design of the joint is critical. Selection of the specific process requires an understanding of the large number of available options, the variety of possible joint configurations, and the numerous variables that must be specified for each operation.

If the potential benefits of welding are to be obtained and harmful side effects are to be avoided, proper consideration should be given to the selection of the process and the design of the joint.

Generally, the quality of a weld joint is strongly influenced by process parameters during the welding process. In order to achieve high quality welds, a good selection of the process variables should be utilized, which in turn results in

optimizing the bead geometry. The object of this study was to investigate the effect of Gas Metal Arc Welding (GMAW) process variables, joint design parameters on weld bead geometry and joint parameters. With this objective, several steel plates were welded with varying process variables and variety of possible joint configurations. The effect of gap distance, bevel height and heat input were investigated. Results of these studies indicated that numerous process variables of GMAW and variety of possible joint configuration affect the bead geometry, HAZ and weld metal hardness profiles and the amount of discontinuity such as lack of penetration and undercutting.

CHAPTER 2

LITERATURE SURVEY

2.1 Gas Metal Arc Welding

GAS METAL ARC welding (GMAW) is a process that melts and joins metals by heating them with an arc established between a continuously fed filler wire electrode and the metals. The process is used with shielding from an externally supplied gas and without the application of pressure. [1]

In the 1920's, the basic concept of GMAW was introduced. However, it was not commercially available until 1948. At first it was considered to be, fundamentally, a high-current density, small diameter, bare metal electrode process using an inert gas for arc shielding. The primary application of this process was for welding aluminum. As a result, the term MIG (Metal Inert Gas) was used and is still a common reference for the process. Subsequent process developments included operation at low-current densities and pulsed direct current, application to a broader range of materials, and the use of reactive gases (particularly CO_2) and gas mixtures. This latter development has led to formal acceptance of the term gas metal arc welding (GMAW) for the process because both inert and reactive gases are used. [2]

There are two operation modes of GMAW, which are semiautomatic and automatic modes. All commercially important metals such as carbon steel, high-strength low alloy steel, stainless steel, aluminum, copper, titanium and nickel

alloys can be welded in all positions with this process by choosing the appropriate shielding gas, electrode, joint design and welding variables.

2.2 Fundamentals of the Process

A continuous consumable electrode that is shielded by an externally supplied gas is fed automatically in the GMAW process. The process is illustrated in Figure 2.1. After initial settings by the operator, the equipment provides for automatic self-regulation of the electrical characteristics of the arc. Thus, the only manual controls required by the welder for semiautomatic operation are the travel speed and direction, and gun positioning. The arc length and the current (wire feed speed) are automatically maintained with the proper equipment and settings.

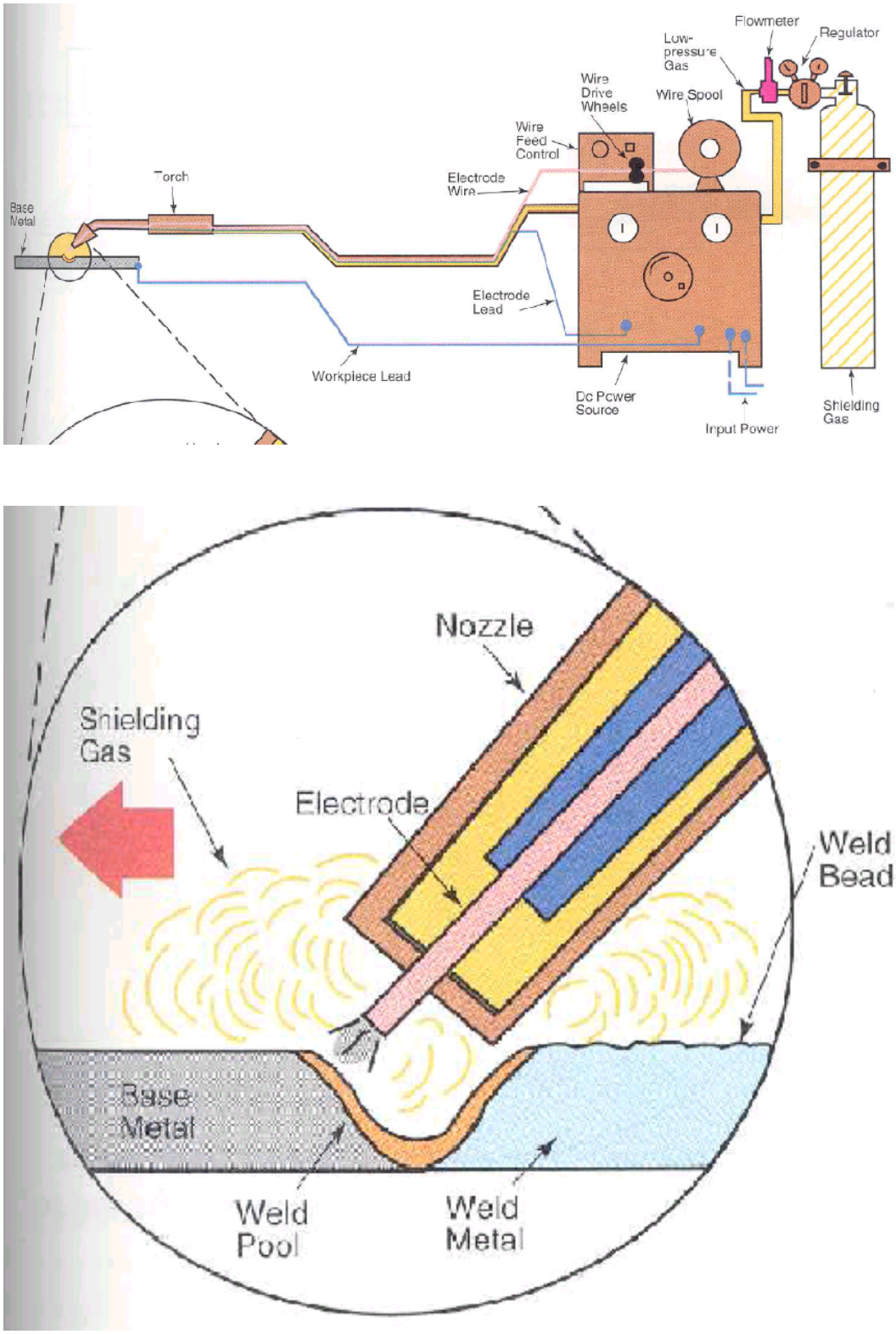

Figure 2.1 Gas Metal Arc Welding Process [6]

2.3 Process Variables

The following are some of the variables that affect weld penetration, bead geometry and overall weld quality:

(1) Welding current (electrode feed speed)
(2) Polarity
(3) Arc voltage (arc length)
(4) Travel speed
(5) Electrode extension
(6) Electrode orientation (trail or lead angle)
(7) Weld joint position
(8) Electrode diameter
(9) Shielding gas composition and flow rate
(10) Metal transfer mechanism

Knowledge and control of these variables is essential to consistently produce welds of satisfactory quality. These variables are not completely independent, and changing one generally requires changing one or more of the others to produce the desired results. Considerable skill and experience are needed to select optimum settings for each application. The optimum values are affected by (1) type of base metal, (2) electrode composition, (3) welding position, (4) quality requirements. Thus, there is no single set of parameters that gives optimum results in every case.

2.3.1 Welding Current

When all other variables are held constant, the welding amperage varies with electrode fed speed or melting rate in a nonlinear relation. As the electrode feed speed is varied, the welding amperage will vary in a like manner if a constant voltage power source is used. This relationship of welding current to wire feed speed for carbon steel electrodes is shown in figure 2.2. At the low-current levels

for each electrode size, the curve is nearly linear. However, at higher welding currents, particularly with small diameter electrodes, the curves become nonlinear, progressively increasing at a higher rate as welding amperage increases. This is attributed to resistance heating of the electrode extension beyond the contact tube. The curves can be approximately represented by the equation [2]

$WFS = aI + bLI^2$

where

WFS = the electrode feed speed, mm/s

a = a constant of proportionality for anode or cathode heating. Its magnitude is dependent upon polarity, composition, and other factors, mm/(s.A)

b = constant of proportionality for electrical resistance heating, $s^{-1}.A^{-2}$

L = the electrode extension or stick out, mm

I = the welding current, A

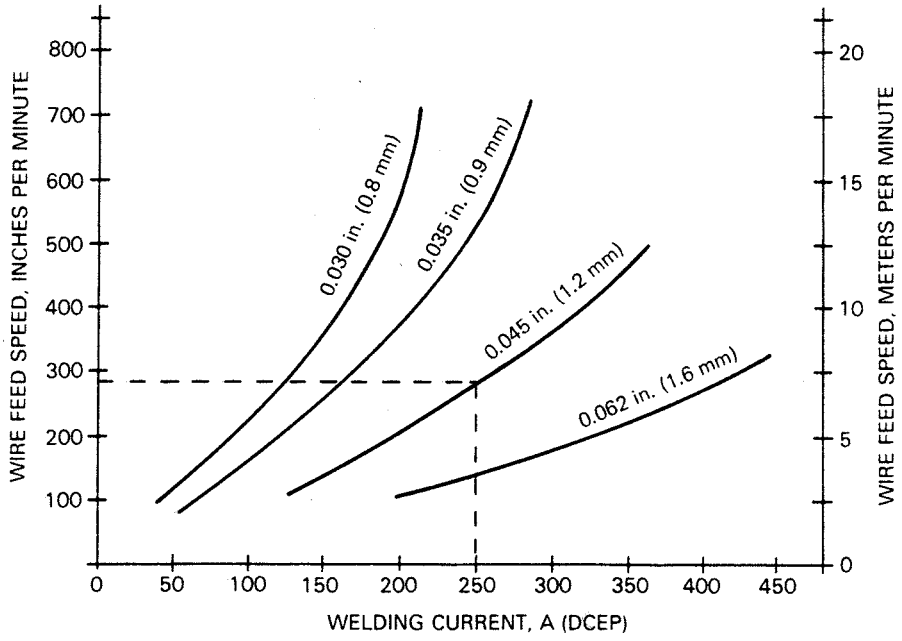

Figure 2.2 Typical welding currents versus wire feed speeds for carbon steel electrodes. [2]

As shown in Figure 2.2, when the diameter of the electrode is increased (while maintaining the same electrode feed speed), a higher welding current is required. The relationship between the electrode feed speed and the welding current is affected by the electrode chemical composition

With all other variables held constant, an increase in welding current (electrode feed speed) will result in the following:

(1) An increase in the depth and width of the weld penetration
(2) An increase in the deposition rate
(3) An increase in the size of the weld bead

2.3.2 Polarity

The term polarity is used to describe the electrical connection of the welding gun with relation to the terminals of a direct current power source. When the gun power lead is connected to the positive terminal, the polarity is designated as direct current electrode positive (DCEP), arbitrarily called reverse polarity. When the gun is connected to the negative terminal, the polarity is designated as direct current electrode negative (DCEN), originally called straight polarity. The vast majority of GMAW applications use direct current electrode positive (DCEP). This condition yields a stable arc, smooth metal transfer, relatively low spatter, good weld bead characteristics and greatest depth of penetration for a wide range of welding currents. [2]

Direct current electrode negative (DCEN) is seldom used because axial spray transfer is not possible without modifications that have had little commercial acceptance. DCEN has a distinct advantage of high melting rates that can not be exploited because the transfer is globular. With steels, the transfer can be improved by adding a minimum of 5 percent oxygen to the argon shield (requiring special alloys to compensate for oxidation losses) In this case, the

deposition rates drop, eliminating the only real advantage of changing polarity. However, because of the high deposition rate and reduced penetration, DCEN has found some use in surfacing applications.

Attempts to use alternating current with the GMAW process have generally been unsuccessful. The cyclic waveform creates arc instability due to tendency of the arc to extinguish as the current passes through the zero point. Although special wire surface treatments have been developed to overcome this problem, the expense of applying them has made the technique uneconomical. [3]

2.3.3 Arc Voltage (Arc Length)

Arc voltage and arc length are terms that are often used interchangeably. It should be pointed out, however, that they are different even though they are related. With GMAW, arc length is a critical variable that must be carefully controlled. For example, in the spray-arc mode with argon shielding, an arc that is too short experiences momentary short circuits. They cause pressure fluctuations, which pump air into the arc stream, producing porosity or embrittlement due to absorbed nitrogen. Should the arc be too long, it tends to wander, affecting both the penetration and surface bead profiles. A long arc can also disrupt the gas shield. In the case of buried arcs results in excessive spatter as well as porosity; if the arc is too short, the electrode tip short circuits the weld pool, causing instability. [2]

Arc length is the independent variable. Arc voltage depends on the arc length as well as many other variables, such as the electrode composition and dimensions, the shield gas, the welding technique and, since it often is measured at the power supply, even the length of the welding cable. Arc voltage is an approximate means of stating the physical arc length (see figure 2.3) in electrical terms, although the arc voltage also includes the voltage drop in the electrode extension beyond the contact tube.

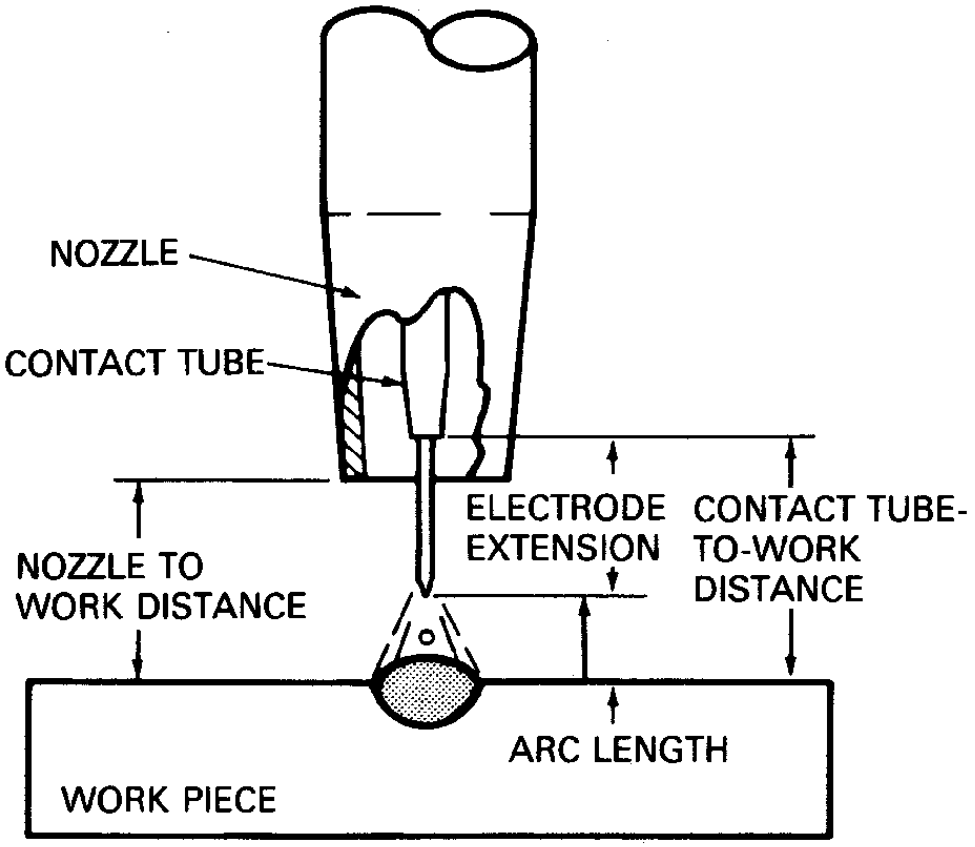

Figure 2.3 Gas metal arc welding terminology [2]

With all variables held constant, arc voltage is directly related to arc length. Even though the arc length is the variable of interest and the variable that should be controlled, the voltage is more easily monitored. Because of this, and the normal requirement that the arc voltage be specified in the welding procedure, it is the term that is more commonly used.

Arc voltage settings vary depending on the material, shielding gas, and transfer mode. Trial runs are necessary to adjust the arc voltage to produce the most favorable arc characteristics and weld bead appearance. Trials are essential because the optimum arc voltage is dependent upon a variety of factors, including

metal thickness, the type of joint, welding position, electrode size, shielding gas composition, and the type of weld. From any specific value of arc voltage, a voltage increase tends to flatten the weld bead and increase the width of the fusion zone. Excessively high voltage may cause porosity, spatter, and undercut. Reduction in voltage results in a narrower weld bead with a higher crown and deeper penetration. Excessively low voltage may cause stubbing of the electrode.

2.3.4 Travel Speed

Travel speed is the linear rate at which the arc is moved along the weld joint. With all other conditions held constant, weld penetration is maximum at an intermediate travel speed.

When the travel speed is decreased, the filler metal deposition per unit length increases. At very low speeds the welding arc impinges on the molten weld pool, rather than the base metal, thereby reducing the effective penetration. A wide weld bead is also a result. [2]

As the travel speed is increased, the thermal energy per unit length of weld transmitted to the base metal from the arc is at first increased, because the arc acts more directly on the base metal. With further increase in travel speed, less thermal energy per unit length of weld is imparted to the base metal. Therefore, melting of the base metal first increases and then decreases with increasing travel speed. As travel speed is increased further, there is tendency toward undercutting along the edges of the weld bead because there is insufficient deposition of filler metal to fill the path melted by the arc. [2]

2.3.5 Electrode Extension

The electrode extension is the distance between the end of the contact tube and the end of the electrode, as shown in figure 2.3. An increase in the electrode extension

results in an increase in its electrical resistance. Resistance heating in turn causes the electrode temperature to rise, and results in a small increase in electrode melting rate. Overall, the increased electrical resistance produces a greater voltage drop from the contact tube to the work. This is sensed by the power source, which compensates by decreasing the current. That immediately reduces the electrode-melting rate, which then lets the electrode shorten the physical arc length. Thus unless there is an increase in the voltage at the welding machine, the filler metal will be deposited as a narrow, high-crowned weld bead. [3]

The desirable electrode extension is generally from 6 to 13 mm for short circuiting transfer and from 13 to 25 mm for other types of metal transfer. [2]

2.3.6 Electrode Orientation

As with all arc welding processes, the orientation of the welding electrode with respect to the weld joint affects the weld bead shape and penetration. Electrode orientation affects bead shape and penetration to a greater extent than arc voltage or travel speed. The electrode orientation is described in two ways: (1) by the relationship of the electrode axis with respect to the direction of travel (the travel angle), and (2) the angle between the electrode axis and the adjacent work surface (work angle). When the electrode points opposite from the direction of travel, the technique is called backhand welding with a drag angle. When the electrode points in the direction of travel, the technique is forehand welding with a lead angle. The electrode orientation and its effect on the width and penetration of the weld are illustrated in Figures 2.4 (A), (B), and (C).

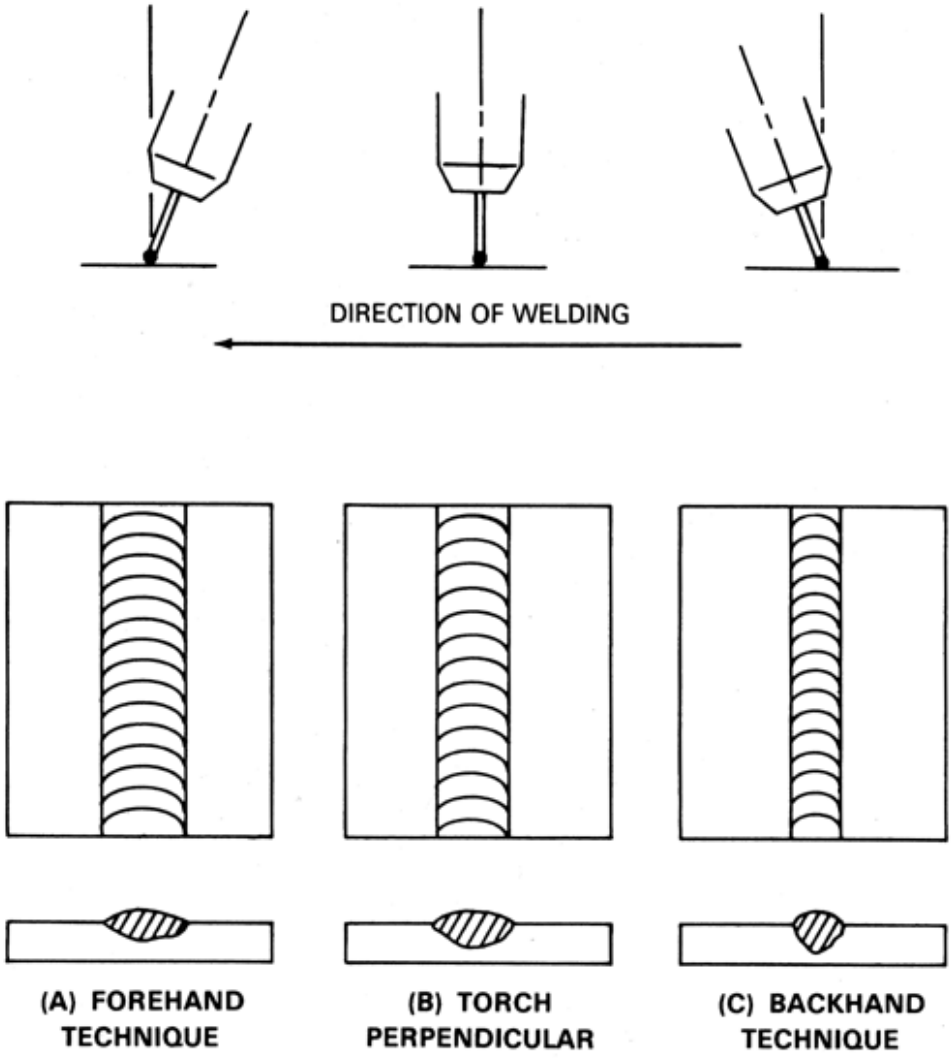

Figure2.4 Effect of electrode position and welding technique [2]

When the electrode is changed from the perpendicular to a lead angle technique with all other conditions unchanged, the penetration decreases and the weld bead become wider and flatter. Maximum penetration is obtained in the flat position with the drag technique, at a drag angle of about 25 degrees from perpendicular. The drag technique also produces a more convex, narrower bead, amore stable arc, and less spatter on the workpiece. For all positions, the electrode travel angle normally used is a drag angle in the range of 5 to 15 degrees for good control and shielding of the molten weld pool. [2]

2.3.7 Electrode Size

The electrode size (diameter) influences the weld bead configuration. A larger electrode requires higher minimum current than a smaller electrode for the same metal transfer characteristics. Higher currents in turn produce additional electrode melting and larger, more fluid weld deposits. Higher currents also result in higher deposition rates and greater penetration. [3]

2.3.8 Shielding Gases

The primary function of the shielding gas is to exclude the atmosphere from contact with molten weld metal. This is necessary because most metals, when heated to their melting point in air, exhibit a strong tendency to form oxides and, to a lesser extent, nitrides. Oxygen will also react with carbon in molten steel to form carbon monoxide and carbon dioxide. These varied reaction products may result in weld deficiencies, such as trapped slag, porosity, and weld metal embrittlement. Reaction products are easily formed in the atmosphere unless precautions are taken to exclude nitrogen and oxygen.

Initially, shielding gases were used to avoid weld pool contamination by oxygen, nitrogen and air humidity by using inert gas such as argon and helium. However, the protection of the weld pool is not the only criterion for selecting a shielding gas. Factors like arc stability, metal transfer, penetration and weld bead profile, tendency for undercutting, cleaning action and welding speed are also influenced by the shielding gas.

Properly selected, a shielding gas can make welding easy and fast, it can control bead contour, and it can even help to control deposit chemistry, penetration and weld defects.

Argon, helium and mixtures of the two can be used for welding virtually any metal but are used primarily with the nonferrous metals. The arc energy is less uniformly dispersed in an argon arc than in helium arc because of the lower thermal conductivity of argon. Consequently, the argon arc plasma has a very high energy core and an outer mantle of lesser thermal energy. This helps produce a stable, axial transfer of metal droplets through an argon arc plasma. The resultant weld cross section is characterized by “argon finger” type penetration pattern such as shown in figure 2.5. With pure helium shielding, on the other hand, a broad, parabolic-type penetration is often observed. [1]

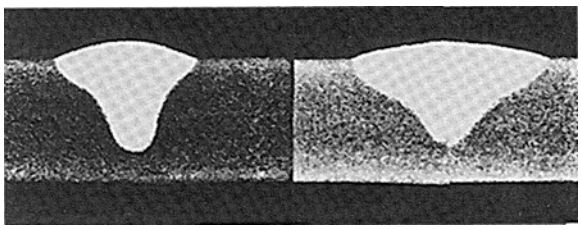

Figure 2.5 Gas-metal arc welds with argon(left) and 75% He-25% Ar (right) [1]

With ferrous metals, however, helium shielding may produce spatter and argon shielding may cause undercutting at the fusion lines. Adding oxygen (about 3%) or carbon dioxide (about 9%) to argon reduces the problems. Carbon and low alloy steels are often welded with carbon dioxide as the shielding gas, the advantages being higher welding speed, greater penetration, and lower cost. Since carbon dioxide shielding produces a high level of spatter, a relatively low voltage is used to maintain a short buried arc to minimize spatter; that is the electrode tip is actually below the workpiece surface. [1]

2.3.9 Equipment

GMAW welding system includes mainly a welding power supply, a wire feed unit, appropriate hoses, a gas supply, a regulator, and according to the amperage, a water-cooling unit. (Figure 2.1)

The range of voltage across the welding arc changes from 17 (which is the minimum voltage to start an arc) to approximately 45 volts. The range of current that can be supplied through the power source changes from 10 amperes to 1500 amperes or more.

The major power supply used in GMAW welding is DCRP (direct current reverse polarity). The major types of machines used to supply DCRP to the system are the DC generator and AC rectifier transformers. The GMAW welding machine must produce either a constant-arc voltage(CAV) or a rising-arc voltage (RAV). The CAV was the first type of voltage amperage characteristics used in GMAW welding machines.

In order to obtain a neat weld bead, the length of the arc must be constant. This can be obtained by a power source, which has a CAV characteristic. During welding, under normal circumstances, there is equilibrium between the melting rate of an electrode and electrode feed rate. In the case of any deviation from this equilibrium condition, i.e. if the distance between the workpiece and welding gun increases (holding the welding gun up) the power source respond instantaneously and try to maintain the initial distance. So, arc length increases which cause a slight increase in the voltage and a sharp decrease in current. This decrease in current decreases the melting rate of an electrode. Hence, again an equilibrium condition is established. Similarly, if the distance between the workpiece and welding gun decreases (holding the welding gun down), arc length decreases which cause a slight decrease in the voltage and a sharp increase in current. This increase in current increases the melting rate of an electrode. Hence, again an equilibrium condition is established.

2.3.9.1 Electrode Feed Unit

The electrode feed unit (wire feeder) consists of an electric motor, drive rolls, and accessories for maintaining electrode alignment. These units can be integrated with the speed control or located remotely from it. The electrode feed motor pushes the electrode through the gun to the work. [2]

2.3.10 Metal Transfer Mechanisms

The molten metal at the electrode tip can be transferred to the weld pool by three basic transfer modes:

(1) Short circuiting transfer
(2) Globular transfer
(3) Spray transfer

The type of transfer is determined by a number of factors, the most influential of which are the following:

(1) Magnitude and type of welding current
(2) Electrode diameter
(3) Electrode composition
(4) Electrode extension
(5) Shielding gas

2.3.10.1 Short Circuiting Transfer

The molten metal at the electrode tip is transferred from the electrode to the weld pool when it touches the pool surface, that is, when short-circuiting occurs. No metal is transferred across the arc gap. Short-circuiting transfer encompasses the lowest range of welding currents and electrode diameters. It produces a small, fast-freezing weld pool that is desirable for joining thin sections, for out-of-

position welding (such as overhead-position welding), and for bridging large root openings. [1]

The electrode contacts the molten weld pool in a range of 20 to over 200 times per second. The sequence of events in the transfer of metal and the corresponding current and voltage are shown in Figure 2.6. As the wire touches the weld metal, the current increases [(A), (B), (C), (D)] in figure 2.6] The molten metal at the wire tip pinches off at D and E, initiating an arc as shown in (E) and (F). The rate of current increase must be high enough to heat the electrode and promote metal transfer, yet low enough to minimize spatter caused by violent separation of the drop of metal. This rate of current increase is controlled by adjustment of the inductance in the power source.

The optimum inductance setting depends on both the electrical resistance of the welding circuit and the melting temperature of the electrode. When the arc is established, the wire melts at the tip as the wire is fed forward towards the next short circuit at (H), Figure 2.6. The open circuit voltage of the power source must be so low that the drop of molten metal at the wire tip cannot transfer until it touches the base metal. The energy for arc maintenance is partly provided by energy stored in the inductor during the period of short-circuiting.

Even though metal transfer occurs only during short-circuiting, shielding gas composition has a dramatic effect on the molten metal surface tension. Changes in shielding gas composition may dramatically affect the drop size and the duration of the short-circuit. In addition, the type of gas influences the operating characteristics of the arc and base metal penetration. Carbon dioxide generally produces high spatter levels compared to inert gases, but CO_2 also promotes deeper penetration. To achieve a good compromise between spatter and penetration, mixtures of CO_2 and argon are often used when welding carbon and low alloy steels. Additions of helium to argon increase penetration on nonferrous metals. [2]

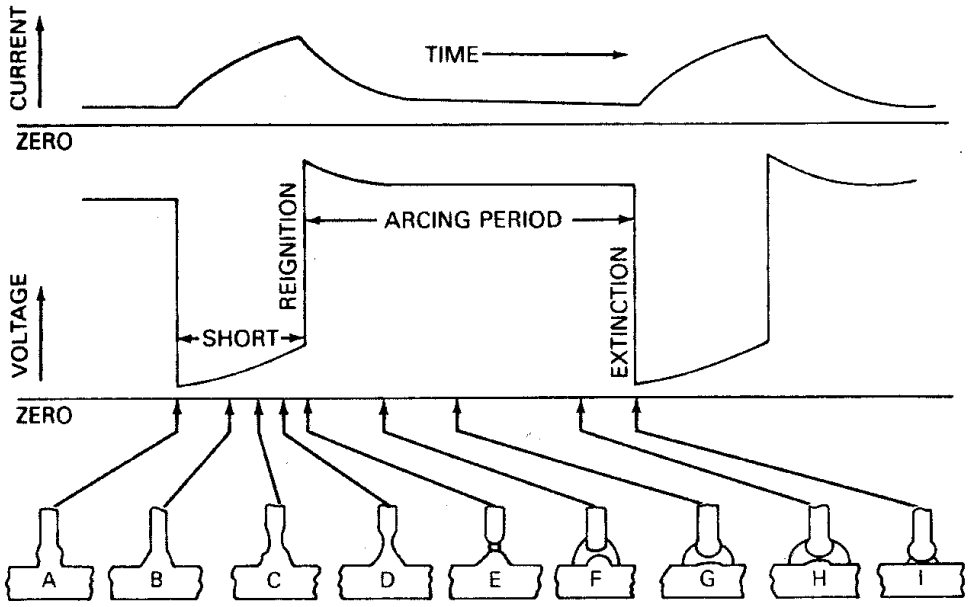

Figure 2.6 Schematic representation of short-circuiting metal transfer [2]

2.3.10.2 Globular Transfer

Discrete metal drops close to or larger than the electrode diameter travel across the arc gap under the influence of gravity. At relatively low welding current globular transfer occurs regardless of the type of shielding gas. With carbon dioxide and helium, however, it occurs at all usable welding currents. [1]

At average currents, only slightly higher than those used in short circuiting transfer, globular axially-directed transfer can be achieved in a substantially inert gas shield. If the arc length is too short (low voltage), the enlarging drop may short to the workpiece, become superheated, and disintegrate, producing considerable spatter. The arc must therefore be long enough to ensure detachment of the drop before it contacts the weld pool. However, a weld made using the higher voltage is likely to be unacceptable because of lack of fusion, insufficient

penetration, and excessive reinforcement. This greatly limits use of the globular transfer mode in production application.

Carbon dioxide shielding results in randomly directed globular transfer when the welding current and voltage are significantly above the range of short circuiting transfer. The departure from axial transfer motion is governed by electromagnetic forces, generated by the welding current acting upon the molten tip as shown in Figure 2.7. The most important of these are the electromagnetic pinch force (*P*) and anode reaction force (*R*). [2]

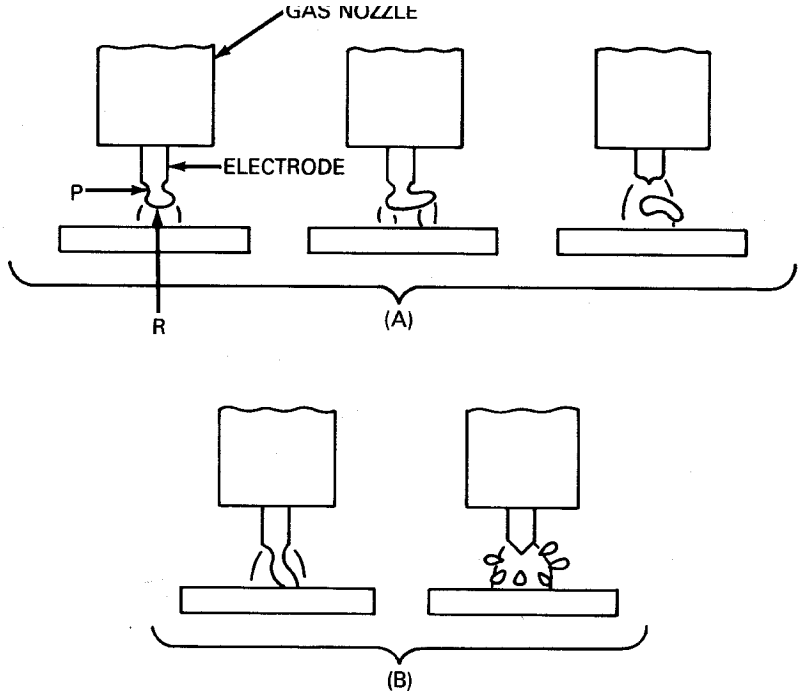

Figure2.7 Non axial globular transfer [2]

The magnitude of the pinch force is a direct function of welding current and wire diameter, and is usually responsible for drop detachment. With CO_2 shielding, the welding current is conducted through the molten drop and the electrode tip is not enveloped by the arc plasma. High speed photography shows that the arc moves

over the surface of the molten drop and workpiece, because force R tends to support the drop. The molten drop grows until it detaches by short circuiting (Figure 2.7B) or by gravity (Figure 2.7A), because R is never overcame by P alone. As shown in figure 2.7A, it is possible for the drop to become detached and transfer to the weld pool without disruption. The most likely situation is shown in figure 2.7B, which shows the drop short circuiting the arc column and exploding. Spatter can therefore be severe, which limits the use of CO_2 shielding for many commercial applications.

Nevertheless, CO_2 remains the most commonly used gas for welding mild steels. The reason for this is that the spatter problem can be reduced significantly by "burying" the arc. In so doing, the arc atmosphere becomes a mixture of the gas and iron vapor, allowing the transfer to become almost spraylike. The arc forces are sufficient to maintain depressed cavity, which traps much of the spatter. This technique requires higher welding current and results in deep penetration. However, unless the travel speed is carefully controlled, poor wetting action may result in excessive weld reinforcement. [2]

2.3.10.3 Spray Transfer

With argon-rich shielding it is possible to produce a very stable, spatter-free "axial spray" transfer mode as illustrated in figure 2.8. This requires the use of direct current and a positive electrode (DCEP), and a current level above a critical value called the transition current. Below this current, transfer occurs in the globular mode, at the rate of a few drops per second. Above the transition current, the transfer occurs in the form of very small drops that are formed and detached at the rate of hundreds per second. They are accelerated axially across the arc gap. The relationship between transfer rate and current is plotted in Figure 2.8. [2]

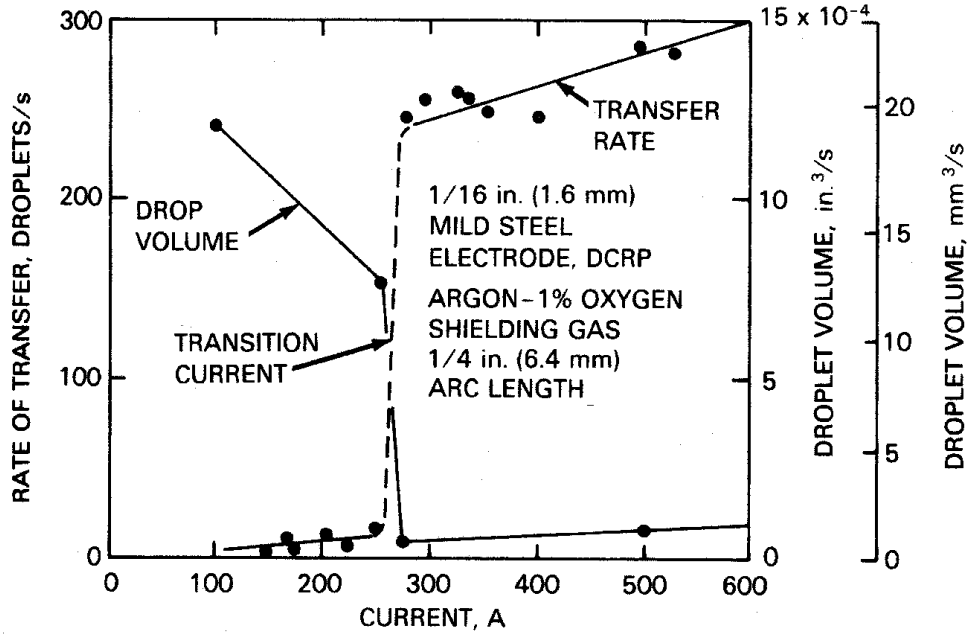

Figure 2.8 Variation in volume and transfer rate of drops with welding current (Steel electrode) [2]

The transition current, which is dependent on the liquid metal surface tension, is inversely proportional to the electrode diameter and, to a smaller degree, to the electrode extension. It varies with the filler metal melting temperature and shielding gas composition.

The spray transfer mode results in a highly directed stream of discrete drops that are accelerated by arc forces to velocities, which overcome the effects of gravity. Because of that, the process, under certain conditions, can be used in any position. Because the drops are smaller than arc length, short circuits do not occur, and spatter is negligible if not totally eliminated.

Another characteristics of the spray mode of transfer is the “finger” penetration which it produces. Although the finger can be deep, it is affected by magnetic

fields, which must be controlled to keep it located at the center of the weld penetration profile.

The spray-arc transfer mode can be used to weld almost any metal or alloy because of inert characteristics of the argon shield. However, applying the process to thin sheets may be difficult because of high currents needed to produce spray arc. The resultant arc forces can cut through relatively thin sheets instead of welding them. Also, the characteristically high deposition rate may produce a weld pool too large to be supported by surface tension in the vertical or overhead position. [2]

CHAPTER 3

EXPERIMENTAL

3.1 Materials Used

Chemical composition of the base metals, filler metal and shielding gas used in the experiments is given below. These materials were selected because of their availability and wide usage in the industry.

3.1.1 Base Metals

Probably the most important factor relating to the weldability of steels is their chemical composition. ” The term weldability has no universally accepted meaning and the interpretation placed upon the term varies widely according to individual viewpoint. The American Welding Society defines weldability as the capacity of a metal to be welded under the fabrication conditions imposed, into a specific, suitably designed structure, and to perform satisfactorily in the intended service. ” [4]

During the experiments carbon and low alloyed steel plates were used. S235 with the dimensions of 4x50x200 mm is selected to represent the carbon steels and recognized as low carbon steels since it contains carbon as an alloying element in quantities not over 0.30%. The chemical composition of S235 is given at Table 3.1

Table 3.1 Chemical compositions of S235 and 31CrV3

Alloy designation	Chemical composition, max wt%										
	%C	%Si	%Mn	%P	%S	%Cr	%Mo	%Ni	%V	%Al	%Cu
31CrV3	0.33	0.27	0.50	0.011	0.029	0.55	0.01	0.08	0.09	0.030	0.20
S235	0.22	0.50	1.60	0.050	0.050	-	-	-	-	-	-

"The weldability of carbon steel, discounting such factors as thickness and joint geometry, is a function of the carbon content. All carbon steels can be welded by metal-arc welding. Where the carbon content does not exceed 0.30 to 0.35%, depending on the thickness of the material, this material can be welded by any procedure which will assure proper penetration and fusion". [5]

In order to represent the low alloyed steels, 31CrV3 steel plate with the dimensions of 6.5x55x100 mm is selected and its composition is given at Table 3.1.

3.1.2 Filler Metal

"The majority of arc welding is done with the addition of a filler metal that plays a major role in determining the composition and microstructure of the weld. For joining of low carbon and low alloy steels, low carbon low alloy filler metals are usually chosen. They contain less than 0.2% carbon and usually have manganese, silicon, nickel, chromium, vanadium, and molybdenum in various amounts, usually totaling less than 5%. They may also have impurity elements such as phosphorus, sulfur, oxygen, and nitrogen". [4]

Both S235 and 31CrV3 steel plates were welded with using the same filler metal. The selection of the welding wire (or the filler metal) is done according to DIN

EN 440, which specifies requirements for classification of wire electrodes for gas shielded metal arc welding of non alloy and fine grain steels up to 500 N/mm^2 yield strength. [7] G42 G3Si1 with the diameter of 1mm is selected for the experiments. Its composition is given at the Table 3.3.

Table 3.2 Chemical composition of G3Si1

Symbol	Chemical composition, wt%*								
	%C	%Si	%Mn	%P	%S	%Ni	%Mo	%Al	%Ti+%Zr
G3Si1	0.06-0.14	0.70-1.00	1.30-1.60	0.025	0.025	0.15	0.15	0.02	0.15

(*)Single values shown in the table mean maximum values.

3.1.3 Shielding Gas

The main function of the shielding gas is to displace the air in the weld zone and thus prevent contamination of the weld metal by nitrogen, oxygen and water vapor.The selection of the best shielding gas is based on consideration of the material to be welded and type of metal transfer that will be used. According to DIN EN 439 [8] , a shielding gas mixture, M21 is selected for the experiments. It contains 18% CO_2 and 82% Ar.

3.2 Experimental Set-up

The set-up used during the experiments includes shielding gas regulator, welding machine and a Quicky motor which carries and guides the welding gun and travels with the desired constant speeds along the plates to be welded on a 1m long rail system. Figure 3.1 (a), (b) and (c) shows Quicky motor, shielding gas and its regulator and welding machine respectively.

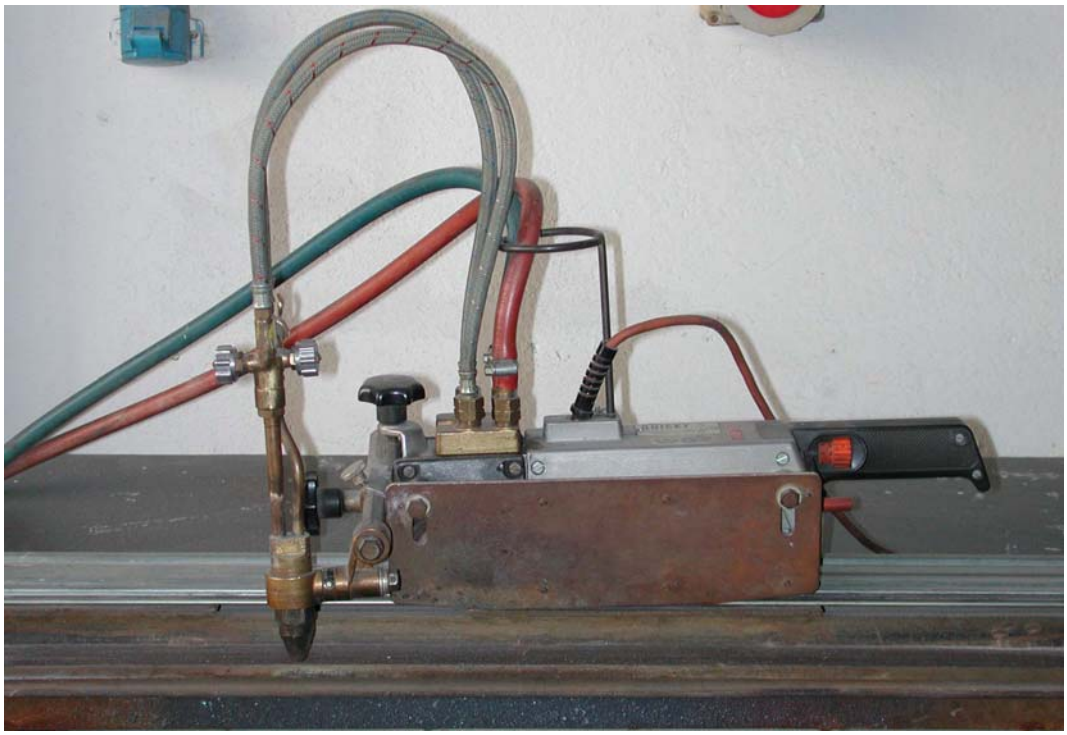

Figure 3.1 (a) Quicky motor

Figure 3.1 (b) Shielding gas and its regulator

Figure 3.1 (c) Welding machine

The motorized unit of the Quicky motor, has an adjustable speed setting ranging from 1 to 10. The calibration of the speed settings was done over 20 cm and converted into corresponding welding speeds. Table 3.4 shows the motor calibration values.

Table 3.3 Motor calibration values

Quicky welding speed setting	2	4	6	8
Corresponding welding speed (cm/sec)	0.40	0.91	1.22	1.54

3.3 Experimental Procedure

3.3.1 Sample preparation

Low carbon steel plates (S235) with the dimensions of 4x50x200 are prepared with the bevel heights of 0, 1, 2, 3 millimeters, bevel angle of 30°. Then, they were tack welded to get a gap distance of 0, 1 and 1.5 millimeters. The dimensions of the weld joint are also given in the table 3.4. Figure 3.2 shows the single V-groove butt joint preparations.

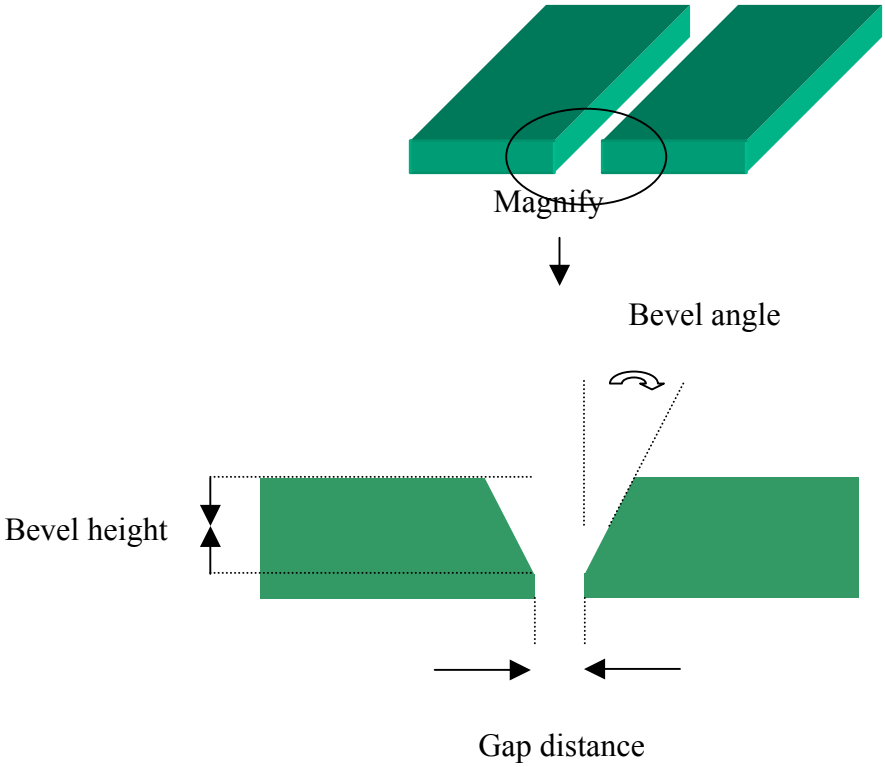

Figure3.2 Single V-groove butt joint preparations

Low alloyed steel plates (31CrV3) with the dimensions of 6.5x55x100 mm are prepared with the bevel height of 3 millimeters, bevel angle of 30° and tack welded to get a gap distance of 0, 1 and 1.5 millimeters. The dimensions of the weld joint are also given in the table 3.4. After proper preparation, plates are placed on the workbench. In each placement, distance between the nozzle and workpiece and the electrode extension were 20 and 10 millimeter, respectively. The orientation of the welding electrode with respect to the weld joint was 90°. After checking the flow rate of shielding gas, which was set to 10 lt/min, welding was started. Both S235 and 31CrV3 were welded at single pass.

Table 3.4 Weld joint dimensions of S235 and 31CrV3.

	S235	31CrV3
Gap distance	0 (zero) mm 1 mm 1.5 mm	0 (zero) mm 1 mm 1.5 mm
Bevel height	0 (zero) mm 1 mm 2 mm 3 mm	3 mm
Bevel angle	30°	

3.3.2 Visual Inspection of the Specimens

Visual inspection is done not only to see the surface of the weld but also get any clues about what is underneath the surface of the weld. Typical weld defects such as spatter “metal particles left after welding, which do not form part of the weld” and undercut “ an irregular groove at a toe of a run in the base metal” [12] can be inspected by this technique. The weld profile, including bead width and height, are measured. In Figure 3.4 the measured bead width and height are given. Table 4.1 tabulates the specimens with corresponding bead width and height.

3.3.3 Metallographic Specimen Preparation

Metallographic specimen preparation was started with sectioning operation. In order to get a representative specimen from the bulk welded specimens, a convenient size which includes the weld metal, HAZ region and base metal is removed by using a wire saw. Mounting operation was not performed since the cut specimens were large enough for handling during preparation and examination. However, sharp edges and corners were eliminated to increase safety and to avoid damage to the papers and cloths used in preparation.

In grinding operation, the section surface was ground using successive finer grades of silicon carbide papers starting from the grit size of 80 and following with 120, 220, 500 and finally 800 grit sizes. Then the surface was polished to remove a surface layer of about 6 : m. At the end, free of scratches, a bright mirror like polished surface was obtained.

In order to reveal the microstructure of a specimen and display the weld bead penetration, etching operation was performed. Nital etchants, containing 10% HNO_3 in ethanol were used which produced successive image contrast for optical examination.

3.3.4 Hardness Test

The Vickers hardness test, which produces relatively small indentations, is used for hardness measurements in transverse cross sections of the specimens. Hardness test was carried out according to the DIN EN 1043-1 [9] , which is the "Hardness test on arc welded joints". A calibrated machine, SHIMADZU HSV 20, forced an indentor of quadrangle geometry under a predetermined load of 10 kg into the surface of the test specimen for test duration of 20 seconds. The resultant impression is expressed as a specific measure of hardness.

The total of 15 indentations have performed from each macrosection of the specimens. Figure 3.3 shows the corresponding regions and the indentation profile on the macrosection of the specimens.

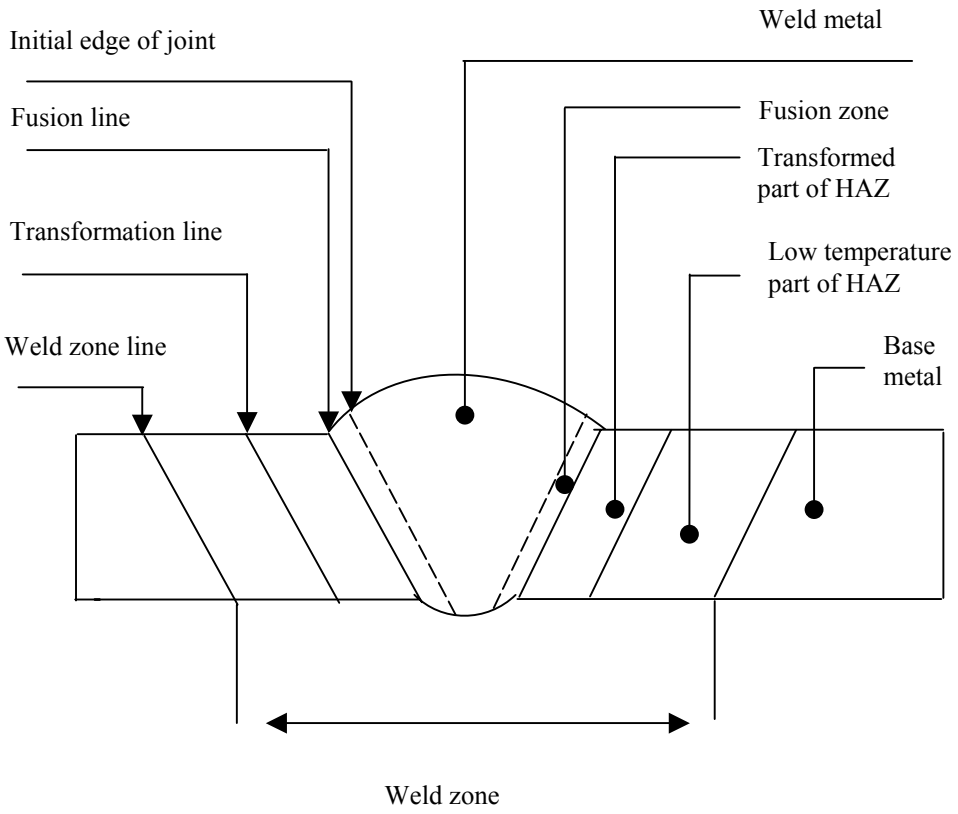

Figure 3.3(a) Corresponding regions of the macrosection of the specimens

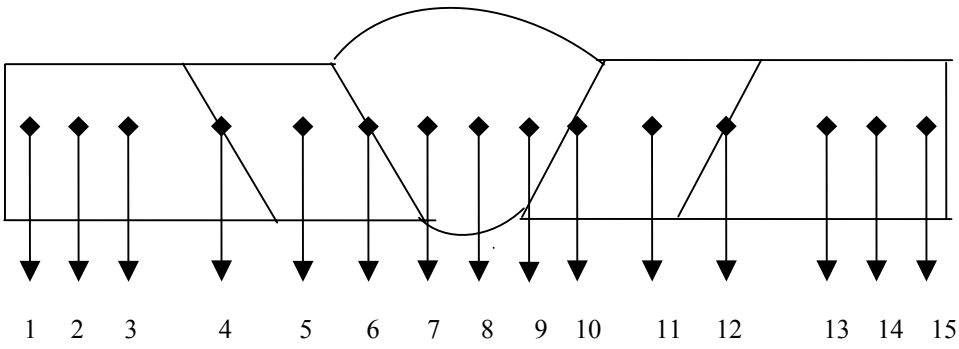

Figure 3.3 (b) Indentation profile on the macrosection of the specimens.

3.3.5 Bead Penetration Measurement

In order to understand the interrelationship between process variables and weld bead penetration, NIKON SMZ-stereo microscope with image magnification of 30X was used to accurately measure the bead penetration on the etched of specimens. Figure 3.4 defines the bead penetration studied.

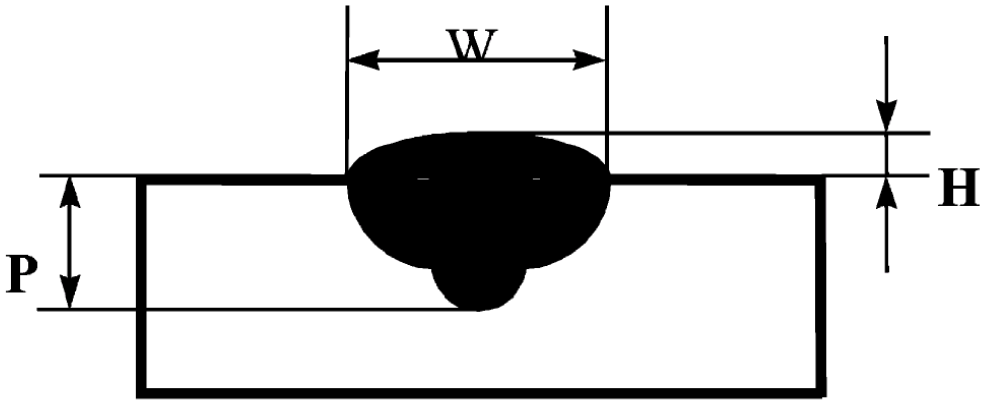

P: Bead penetration

W: Bead width

H: Bead height

Figure 3.4 A schematic diagram for bead penetration, width and height. [13]

3.3.6 Tensile Test

The ultimate tensile strength of the machined specimens were measured in a calibrated HECKERT testing machine which has a capacity of 40 tons. Tensile test was carried out according to the DIN EN 895 [10], which is the "Destructive tests on welds in metallic materials-Transverse tensile test". Figure 3.5 shows the test specimen. Table 3.4 shows the denominations and symbols of the test specimen.

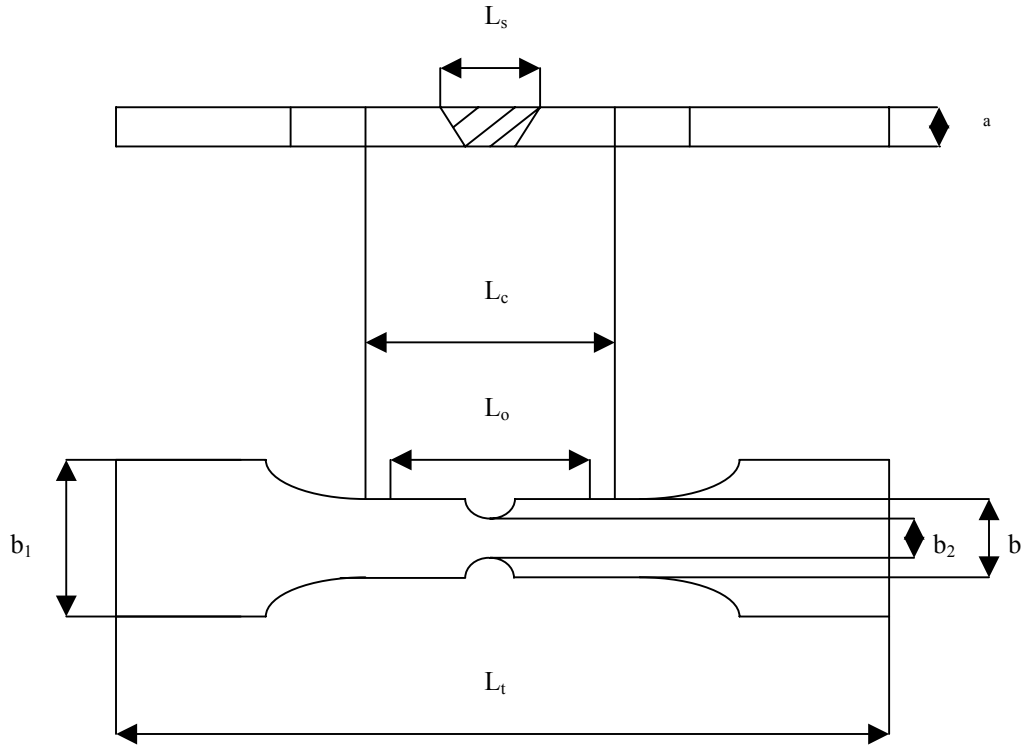

Figure3.5 Tensile Test Specimen [10]

Table 3.5 Denomination and symbols of the tensile test specimen [10]

Symbol	Denomination	Size (mm)
a	Thickness of the test specimen	2
b	Width of the calibrated parallel length	25
b_1	Width of shoulder	37
b_2	Width of the welded joint	15
L_c	Parallel length	70
L_o	Original gauge length	62
L_s	Maximum width of the weld after machining	6
L_t	Total length of the test specimen	100

3.3.7 Dilution Analysis

Dilution is the measurement used to describe the amount of penetration in terms of the base metal. It is described in terms of a percentage of base material within the deposit. [11] In order to find the amount of dilution, chemical analysis was done on the weld metal of the 31CrV3 specimens with the gap distances of 0(zero), 1 and 1.5 millimeters at KOSGEB-OSTİM. Chemical analysis of the base metal was done on the heat number of 030138 at the Çemtaş Steel Plant, BURSA.

$$\% \text{ dilution} = \frac{\text{weight of base metal}}{\text{total weld metal weight}} \times 100\%$$

CHAPTER 4

RESULTS AND DISCUSSION

4.1 Presentation of Results

This study is based on the mechanical properties and cross-sectional characteristics of the MIG-MAG butt welds with varying gap and bevel height distances, and as well as other welding parameters. Low carbon steel plates, S235, were examined with the different welding parameters including bevel height and gap distance. Low alloyed steel plates, 31CrV3, were also examined in the study, however, for comparison. Table 4.1(a) and (b) tabulate the specimens with corresponding welding parameters for S235 and 31CrV3 respectively.

Table 4.1(a)

Specimen no	Gap distance (mm)	Bevel height (mm)	Ampere (A)	Voltage (V)	Travel Speed (cm/s)	Weld bead Height (mm)	Weld bead Width (mm)
A1	1.5	0	130	18	0.4	2.0	6.3
A2	1.5	0	165	18	0.4	2.5	6.7
A3	1.7	0	170	16	0.4	3.1	6.7
A4	2.5	0	180	16	0.4	1.5	6.0
A5	2.2	0	150	16	0.4	2.5	6.2
A6	1.4	0	170	16	0.91	2.0	4.8
A7	1.6	0	170	16	0.91	1.5	4.2
A8	1.5	0	180	16	0.91	1.0	4.1
A9	1.7	0	180	16	0.91	1.5	4.0
A10	2	0	170	16	0.91	1.0	4.8
A11	2	0	170	16	0.91	1.2	4.6
A12	1.6	0	170	15	0.91	2.2	4.0
A13	1.8	0	170	15	0.91	2.1	4.5
A14	1.5	0	140	14	0.91	2.9	4.0

Table 4.1(a) cont'd

Specimen no	Gap distance (mm)	Bevel height (mm)	Ampere (A)	Voltage (V)	Travel Speed (cm/s)	Weld bead Height (mm)	Weld bead Width (mm)
A15	1.7	0	140	14	0.91	5.0	3.3
A16	1.5	0	140	14	0.91	3.0	4.4
A17	2	0	160	16	0.91	1.0	4.8
A18	1.7	0	170	15	1.22	1.0	3.5
A19	2	0	170	15	1.22	1.0	3.5
1	0	0	170	17	0.91	3.0	4.8
2	0	1	170	17	0.91	2.2	4.4
3	0	2	170	17	0.91	2.0	5.3
4	0	3	170	17	0.91	1.5	5.5
5	0	0	170	17	0.91	2.5	5.5
6	0	1	170	17	0.91	2.2	5.0
7	0	2	170	17	0.91	2.2	5.0
8	0	3	170	17	0.91	1.8	4.2
9	1	0	170	17	0.91	2.0	4.8
10	1	1	170	17	0.91	2.2	5.3
11	1	2	170	17	0.91	1.8	5.3
12	1	3	170	17	0.91	1.8	4.7
13	1.5	0	170	17	0.91	1.0	4.4
14	1.5	1	170	17	0.91	1.0	5.2
15	1.5	2	170	17	0.91	1.5	4.4
16	1.5	3	170	17	0.91	1.0	4.6
25	0	0	170	19	0.91	2.4	5.6
26	0	1	170	19	0.91	2.1	5.1
27	0	2	170	19	0.91	2.0	5.2
28	0	3	170	19	0.91	1.7	4.4
29	1	0	170	19	0.91	2.0	4.9
30	1	1	170	19	0.91	2.1	5.6
31	1	2	170	19	0.91	2.1	6.0
32	1	3	170	19	0.91	2.0	6.1
33	1.5	0	170	19	0.91	1.2	6.1
34	1.5	1	170	19	0.91	1.0	6.0
35	1.5	2	170	19	0.91	1.4	4.6
36	1.5	3	170	19	0.91	1.0	4.7
37	0	0	170	22	1.54	1.5	4.8
38	0	1	170	22	1.54	0.8	4.4
39	0	2	170	22	1.54	0.2	6
40	0	3	170	22	1.54	0.5	5.5
41	1	0	170	22	1.54	1.4	4.9
42	1	1	170	22	1.54	0.5	5.1
43	1	2	170	22	1.54	1	5.5
44	1	3	170	22	1.54	0.5	5.4
45	1.5	0	170	22	1.54	0.5	6.4
46	1.5	1	170	22	1.54	0.5	5.6
47	1.5	2	170	22	1.54	0.5	6.2
48	1.5	3	170	22	1.54	0.1	6.4

Table 4.1(b)

Specimen no	Gap distance (mm)	Bevel height (mm)	Ampere (A)	Voltage (V)	Travel Speed (cm/s)
50	0	3	170	19	0.91
51	1	3	170	19	0.91
52	1.5	3	170	19	0.91
53	0	3	170	22	0.91
54	1	3	170	22	0.91
55	1.5	3	170	22	0.91
56	0	3	170	19	0.4
57	1	3	170	19	0.4
58	1.5	3	170	19	0.4
59	0	3	170	22	0.4
60	1	3	170	22	0.4
61	1.5	3	170	22	0.4

The total 48 S235 specimens were visually examined according to the weld bead height and width. The total of nine specimens were selected and metallographically prepared. The selected specimens, tabulated in table 4.2, were compared according to the visual appearances, bead penetrations, hardness values, gap distances, bevel heights and heat inputs. Heat input (Q) was calculated according to the equation(1) below. As can be seen from the table 4.2, voltage values ranges between 14 to 22 volts. Hence, short circuiting transfer mechanism preserved during the experiments.

$$Q\ (J/cm) = \frac{\text{Ampere (A) X Voltage (V)}}{\text{Travel speed (cm/s)}} \qquad (1)$$

Table 4.2 The selected specimens with corresponding process variables.

Heat Input Rate (kJ/cm)	Weld Metal Hardness* (H_V)	HAZ Hardness* (H_V)	Gap Distance (mm)	Bevel Height (mm)	Bead Penetration (mm)	Specimen No
2.42	225	154	0	3	1.76	40
2.42	242	153	1	3	3.71	44
2.42	296	150	1.5	3	4	48
3.18	237	148	0	3	2.62	8
3.18	231	145	1	3	2.75	12
3.18	236	145	1.5	3	4	16
3.55	209	139	1	1	2.24	30
3.55	220	126	1	2	3.04	31
3.55	222	138	1	3	4	32

* HAZ and weld metal hardness values are the average values.

4.2 Effect of heat input rate on hardness

In order to see the effect of heat input on hardness (at constant gap distance over bevel height ratio), specimen 44 with heat input of 2.42 kJ/cm, specimen 12 with heat input of 3.18 kJ/cm and specimen 32 with heat input of 3.55 kJ/cm were compared. All these specimens have gap distance over bevel height ratio of 1/3. The table 4.3 tabulates the fifteen hardness values at each heat input values and figure 4.1 shows the graphical representation of them.

Table 4.3 Hardness values (H_v) at constant gap distance over bevel height ratio.

Specimen no	Heat input	Hardness Indentations														
		1	2	3	4	5	6	7	8	9	10	11	12	13	14	15
44	2.42	104	106	109	137	141	175	227	221	224	169	147	139	118	109	105
12	3.18	113	115	123	141	145	146	231	233	230	150	148	145	114	114	113
32	3.55	107	112	117	138	144	144	230	217	220	147	146	136	118	115	112

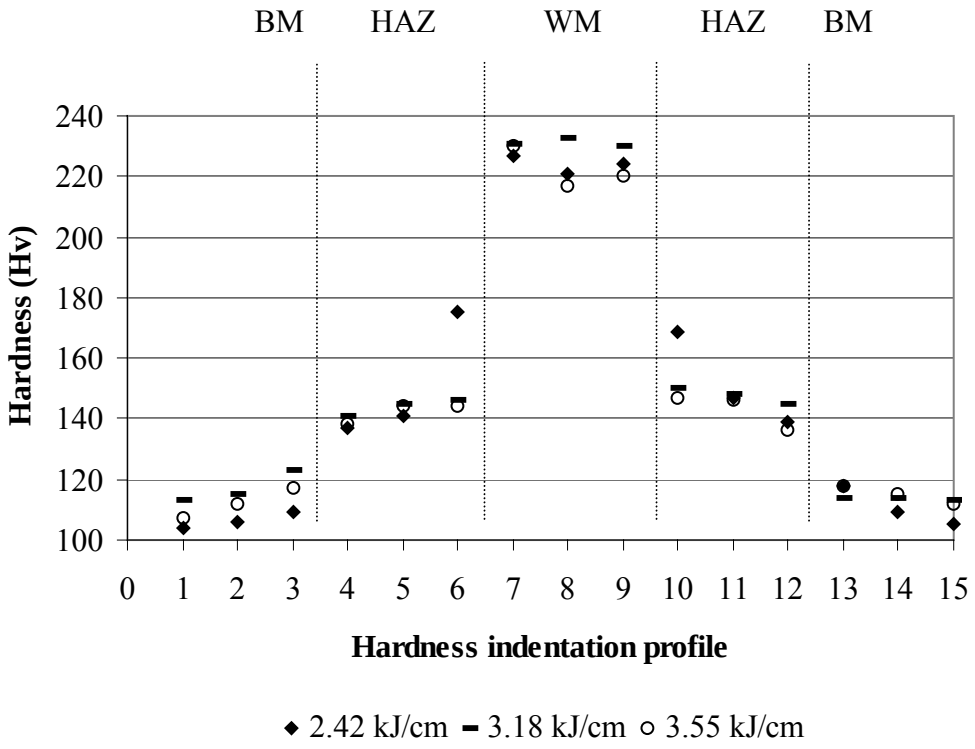

Figure 4.1 Effect of heat input rate on hardness (at constant gap distance over bevel height ratio (1/3))

No significant hardness changes were observed with heat input variation in the weld metal. However, in the heat affected zone, particularly considering the sixth and tenth hardness indentations on the figure 4.1, which correspond to the coarse grains region near the fusion boundary exhibited higher hardness values due to the minimum heat input rate of 2.42 kJ/cm used in the experiments.

4.3 Effect of gap distance on hardness

In order to see the effect of gap distance on hardness (at constant bevel height and heat input), specimens 40, 44 and 48 with heat input of 2.42 kJ/cm and specimens 8, 12 and 16 with heat input 3.18 kJ/cm were compared. The table 4.4 and 4.5 tabulates the fifteen hardness values at each gap distance and figure 4.2 and 4.6 shows the graphical representation of them at corresponding heat input values.

Table 4.4 Hardness values (H_v) at 2.42 kJ/cm

Specimen no	Gap distance	Hardness Indentations														
		1	2	3	4	5	6	7	8	9	10	11	12	13	14	15
40	0	107	108	116	148	148	152	223	222	230	167	159	150	119	118	109
44	1	104	106	109	137	141	175	227	221	224	169	147	139	118	109	105
48	1,5	102	105	108	148	151	157	309	273	306	155	148	139	118	110	106

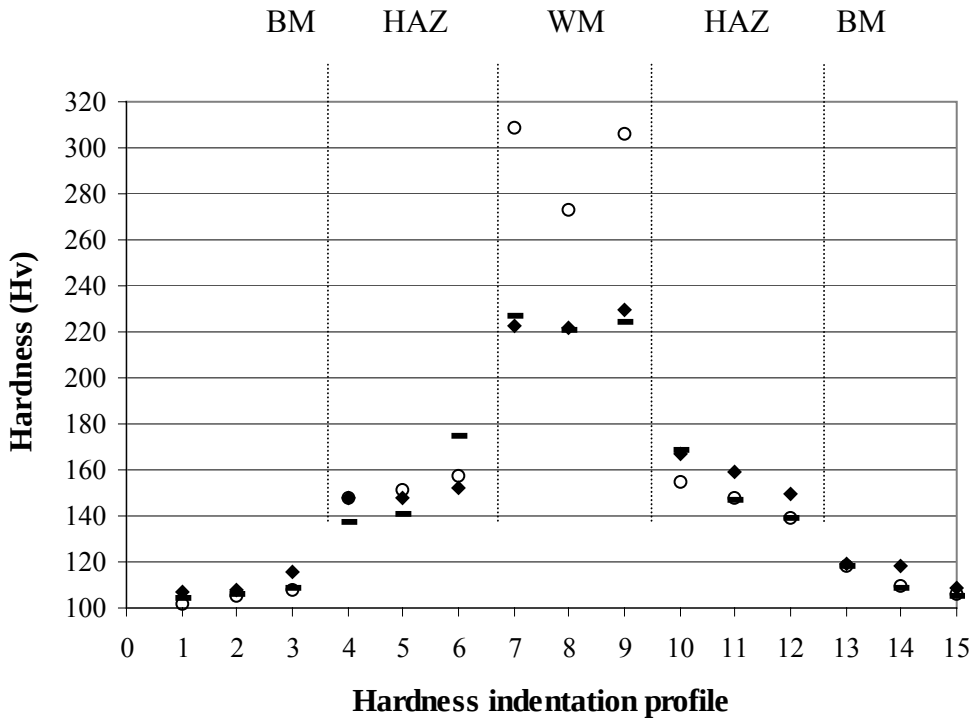

Figure 4.2 Effect of gap distance on hardness (at constant heat input rate, (2.42 kJ/cm) and bevel height (3 mm)).

The visual appearances and macro-photographs of these three specimens, 40, 44 and 48 with the corresponding gap distances at 2.42 kJ/cm are shown at figure 4.3(a&b), 4.4 (a&b) and 4.5(a&b), respectively.

(a)

Large amount of spatter around cap

(b)

No penetration at the root

Figure 4.3 Visual appearance of the specimen 40, both cap (a) and root (b).

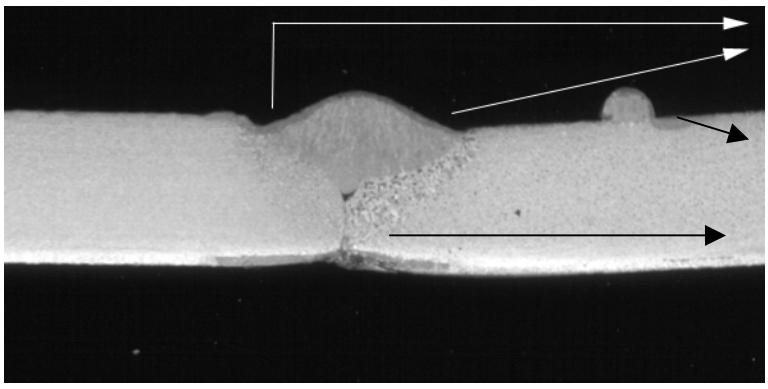

Figure 4.3 (c) Macro-photograph of the specimen 40. (Magnification 5X)

(a)

(b)

Lesser amount of spatter around cap Partial penetration at the root

Figure 4.4 Visual appearances of the specimen 44 cap (a) and root (b).

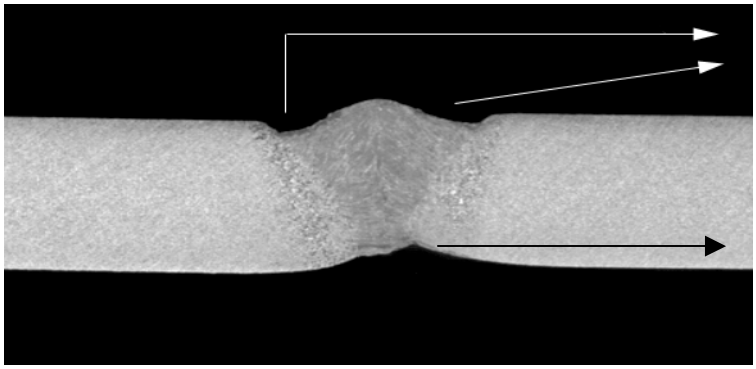

Undercut

Partial penetration

Penetration depth: 3.71 mm

Figure 4.4(c) Macro-photograph of the specimen 44. (Magnification 5X)

(a)

The least amount spatter around cap

(b)

Almost full penetration at the root

Figure 4.5 Visual appearance of the specimen 48 both cap (a) and root (b).

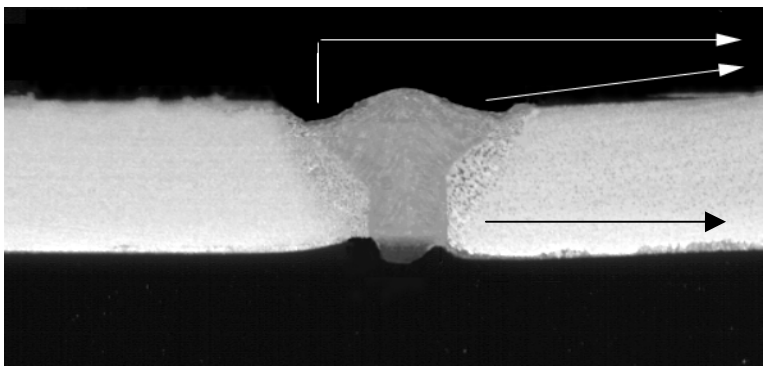

Undercut

Full penetration

Penetration depth: 4.00 mm

Figure 4.5 (c) Macro-photograph of the specimen 48. (Magnification 5X)

Similar to the specimens 40, 44 and 48, specimens 8, 12 and 16 have gap distance of 0,1 and 1.5 millimeters but at 3.18 kJ/cm.

Table 4.5 Hardness values (H_v) at 3.18 kJ/cm.

Specimen no	Gap distance	Hardness Indentations														
		1	2	3	4	5	6	7	8	9	10	11	12	13	14	15
8	0	109	110	116	137	147	155	240	233	238	153	149	148	113	111	111
12	1	113	115	123	141	145	146	231	233	230	150	148	145	114	114	113
16	1.5	115	115	131	143	145	152	244	229	235	145	142	140	117	113	111

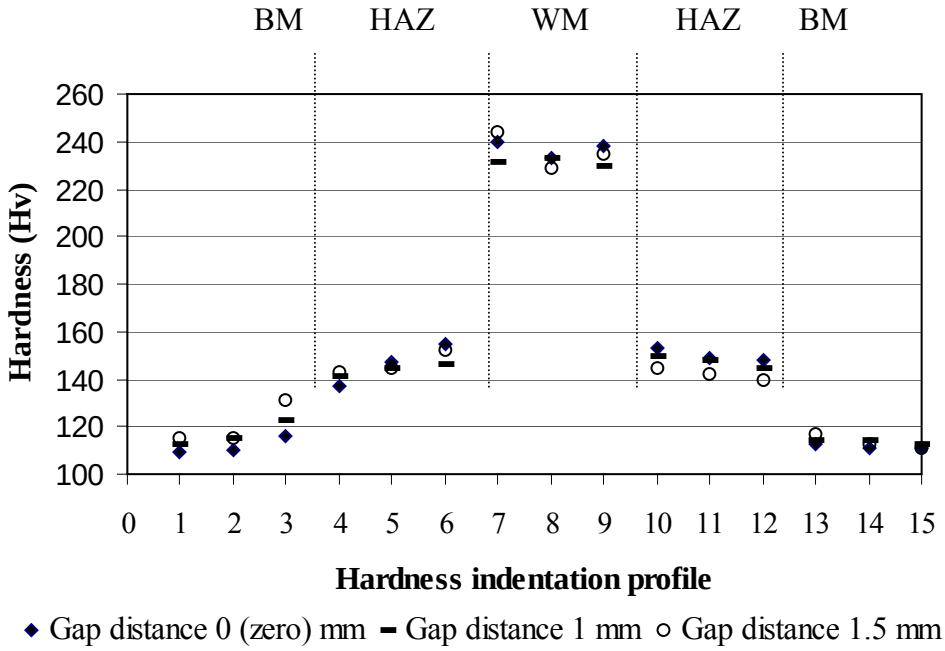

Figure 4.6 Effect of gap distance on hardness (at constant heat input rate, (3.18 kJ/cm) and bevel height (3 mm)).

The visual appearances and Macro-photographs of these three specimens, 8, 12 and 16, with the corresponding gap distances at 3.18 kJ/cm are shown at figure 4.7(a&b), 4.8 (a&b) and 4.9(a&b), respectively.

(a)

Free of spatter

(b)

No penetration at the root

Figure 4.7 Visual appearance of the specimen 8 both cap (a) and root (b).

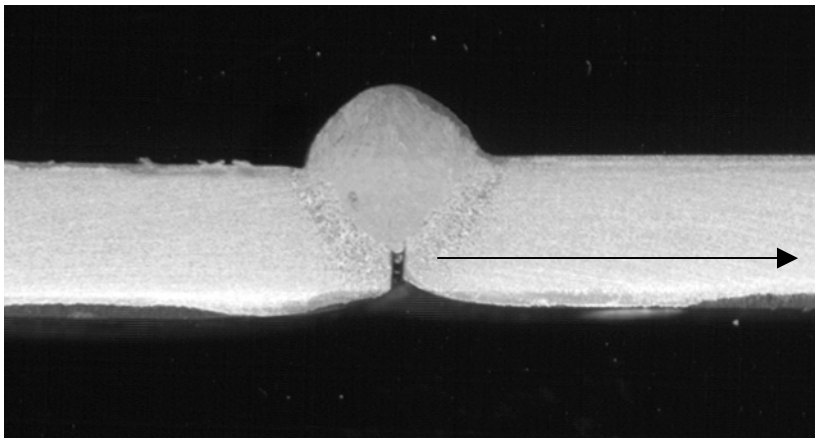

Lack of penetration

Penetration depth: 2.62 mm

Figure 4.7(c) Macro-photograph of the specimen 8. (Magnification 5X)

(a)

Free of spatter

(b)

Partial penetration at the root

Figure 4.8 Visual appearance of the specimen 12 both cap (a) and root (b).

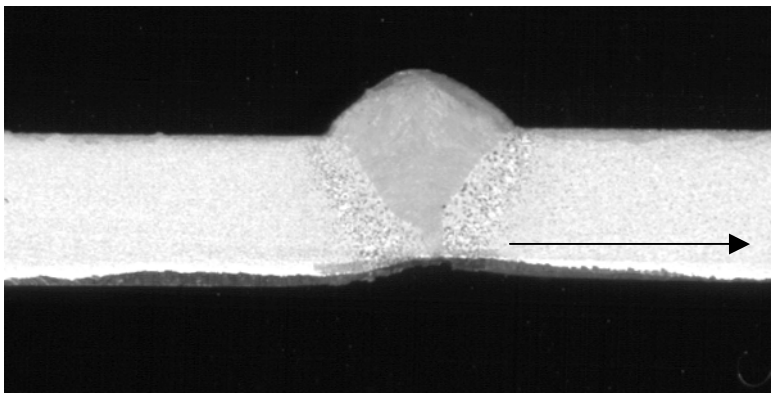

Partial penetration

Penetration depth: 2.75 mm

Figure 4.8 (c) Macro-photograph of the specimen 12. (Magnification 5X)

(a)

Free of spatter

(b)

Full penetration at the root

Figure 4.9 Visual appearance of the specimen 16 both cap (a) and root (b).

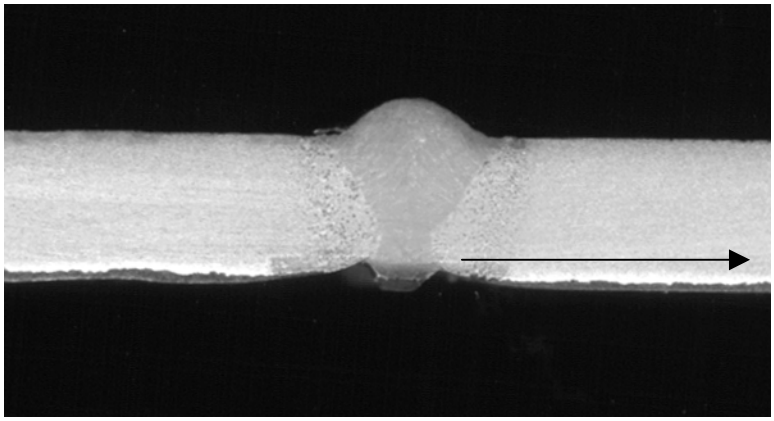

Full penetration

Penetration depth: 4.00 mm

Figure 4.9 (c) Macro-photograph of the specimen 16. (Magnification 5X)

Comparing the visual appearances of the specimens 40, 44 and 48 with specimens 8, 12 and 16, it is seen that specimen 40, 44 and 48 have excessive amount of spatter and undercut. On the other hand, specimens 8, 12 and 16 are free of spatter and undercut

During the experiments, it is also observed that molten metal was running in front of the arc. Since the welding was performed in a semi-automatic system, where the electrode angle with respect to the workpiece was 90°, could not allow any change in the electrode angle to prevent molten metal running in front of the arc.

From the macro-photographs of specimen 40 and 8 both having 0 (zero) millimeters gap distance, it is seen that penetration is very shallow. The measured penetrations are 1.76 and 2.62 millimeters, respectively. Specimens 44 and 12 both having 1 millimeter gap distance, have partial penetration. The measured penetrations are 2.75 and 3.71 millimeters, respectively. Specimen 48 and specimen 16 having 1.5 millimeters gap distance have full penetration of 4 millimeters. However, it should be noticed that the macro-photographs were not representing the whole length of the specimen but only the fifth centimeters of the specimens. Therefore, different penetrations could be measured by sectioning at different lengths of the specimens. As the welding reaches to the end, since the plates will absorb much heat, deeper penetrations could be achieved.

4.4 Effect of bevel height on hardness

In order to see the effect of bevel height on hardness (at constant heat input rate, 3.55 kJ/cm and gap distance, 1 mm), specimen 30 with bevel height of 1 mm, specimen 31 with bevel height of 2 mm and specimen 32 with bevel height of 3 mm were compared. All these specimens have gap distance of 1 mm .The table 4.6 tabulates the fifteen hardness values at each heat input values and figure 4.10 shows the graphical representation of them.

Table 4.6 Hardness values (H_v) at constant gap distance.

Specimen no	Bevel height	Hardness Indentations														
		1	2	3	4	5	6	7	8	9	10	11	12	13	14	15
30	1	116	118	121	138	138	142	208	207	211	145	140	133	119	118	115
31	2	110	112	115	140	140	149	222	216	221	150	138	134	123	119	116
32	3	107	112	117	138	144	144	230	217	220	147	146	136	118	115	112

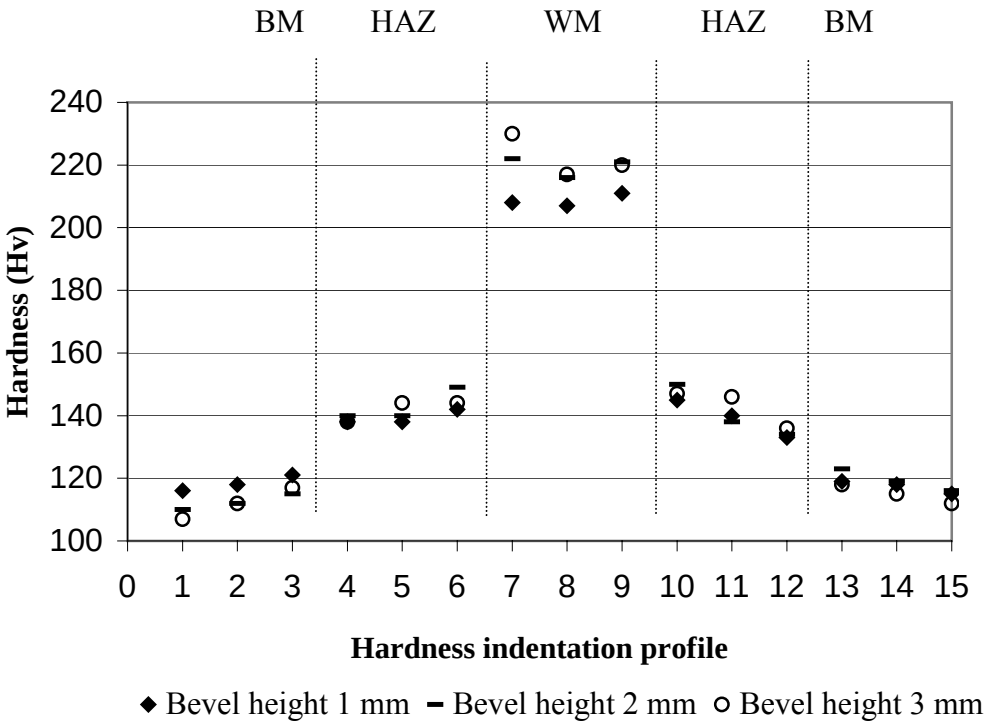

Figure 4.10 Effect of bevel height on hardness (at constant heat input rate, 3.55 kJ/cm and gap distance, 1 mm)

The Macro-photographs of these three specimens, 30, 31 and 32 with the corresponding bevel heights at gap distance of 1mm are shown at figure 4.11, 4.12 and 4.13, respectively.

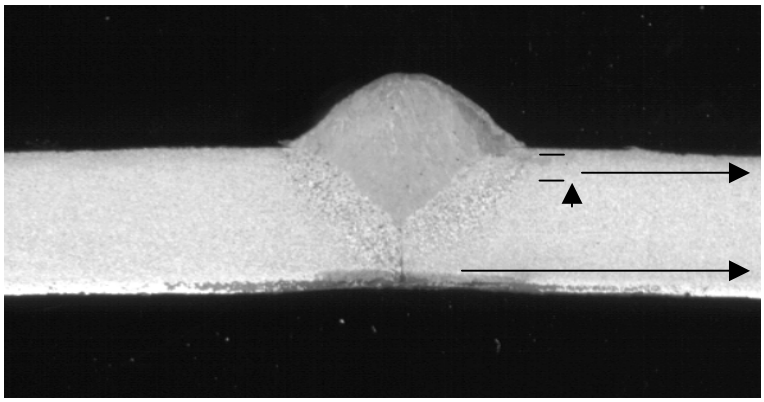

Bevel height : 1 mm
Penetration
depth: 2.24 mm

Figure 4.11 Macro-photograph of the specimen 30. (Magnification 5X)

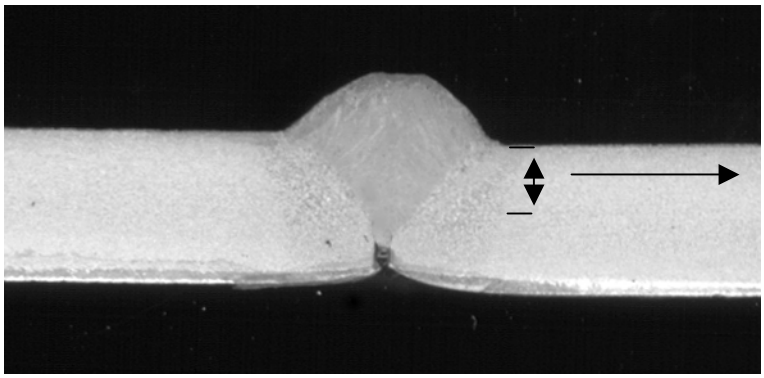

Bevel height : 2 mm
Penetration
depth: 3.04 mm

Figure 4.12 Macro-photograph of the specimen 31. (Magnification 5X)

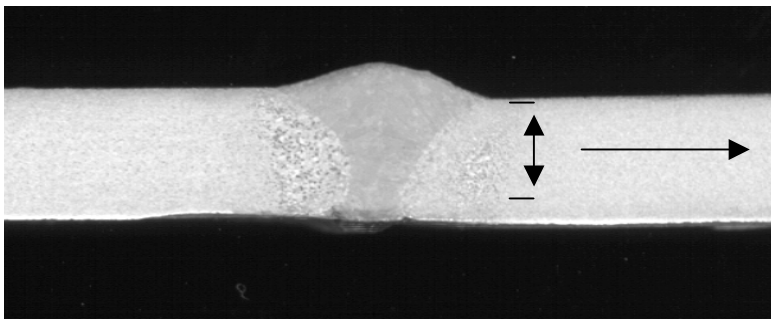

Bevel height : 3 mm
Penetration
depth: 4 mm

Figure 4.13 Macro-photograph of the specimen 32. (Magnification 5X)

From the macro-photographs of specimen 30, 31 and 32, the measured penetrations are 2.24, 3.04 and 4 millimeters respectively. There is a linear correlation with bevel heights (1, 2 and 3 millimeters, respectively) and amount of penetration.

4.5 Effect of gap distance, bevel height and heat input on bead penetration

In order to quantitatively evaluate the effect of process variables on the bead penetration, multiple linear regression analysis was carried out. The following equation (2), with a correlation coefficient (R2) value of 0.80 is obtained.

$$BP = -0.716 + 1.21*(GD) + 0.680*(BH) + 0.003*(HI) \quad (2)$$

where BP is the bead penetration, GD is the gap distance, BH is the bevel height and HI is the heat input. Table 4.7 tabulates the bead penetrations measured from the Macro-photographs and the bead penetrations calculated by the equation given. Figure 4.14 shows the comparison of measured and calculated bead penetration.

As stated earlier, it should be noticed that the bead penetrations are measured at the fifth centimeters of the specimens. Therefore, different penetrations can be measured by sectioning at different lengths of the specimens. Moreover, better penetrations could be achieved if there were any arc oscillation during welding. However, the experiments are performed in a semi-automatic system where the welding gun was carried by Quicky motor on a straight path (no manual control on the welding gun), could not allow any arc oscillation. Arc oscillation, beside its beneficial effect of on penetration, also improves the strength and ductility of the weld. “Kou and Le studied the microstructure in oscillated arc welds of 2014 aluminum alloy. It was observed that the dendrite arm spacing was reduced significantly by transverse arc oscillation at low frequencies, as shown in figure

4.15. This reduction in dendrite arm spacing has contributed to the significant improvement in both the strength and ductility of the weld". [1]

Table 4.7 Bead penetration and the corresponding process variables.

Specimen No	Gap Distance (mm)	Bevel Height (mm)	Heat Input Rate (kJ/cm)	Measured Bead Penetration (mm)	Calculated Bead Penetration (mm)
8	0	3	3.18	2.62	2.51
12	1	3	3.18	2.75	3.45
16	1.5	3	3.18	4	3.90
30	1	1	3.55	2.24	2.28
31	1	2	3.55	3.04	2.98
32	1	3	3.55	4	3.70
40	0	3	2.42	1.76	2.00
44	1	3	2.42	3.71	2.93
48	1.5	3	2.42	4	3.86

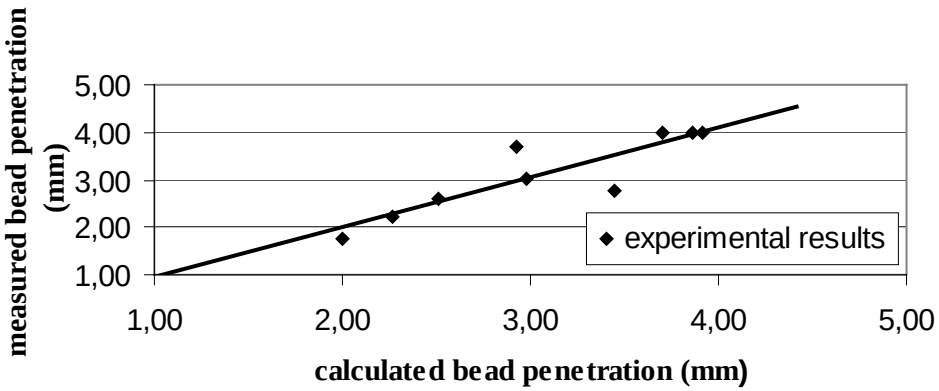

Figure 4.14 Comparison of measured and calculated bead penetration.

The specimen 12 and 32 ,both have the gap distance of 1mm and bevel height of 3 mm and bead penetrations of 2.75 millimeters and 4 millimeters, respectively. This difference is occurred because of the amount of heat input, 3.18 and 3.55 kJ/cm, respectively. Moreover, analyzing the process variables from Table 4.1, it is seen that both specimens were welded at 170 ampere and 0.91 cm/s. The only increase is the voltage, which are 17 and 19 volts, respectively. Gunaraj et al. [15] have also found that the increase in voltage when the rest of process parameters kept constant results in increase in the heat input. As the heat input increases, the depth of penetration increases.

No oscilation Transverse oscilation

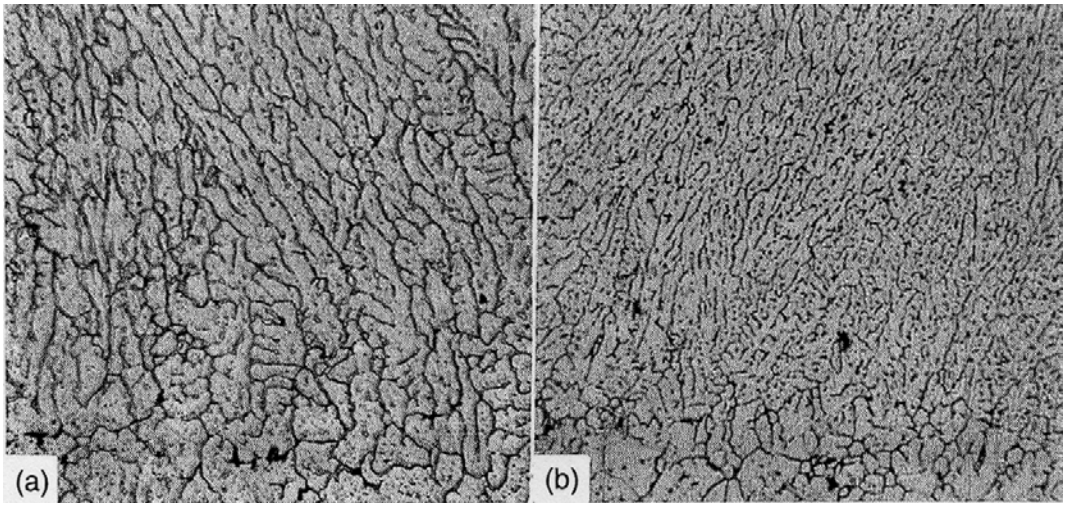

Fig 4.15 Effect of arc oscillation on microstructure (a) coarser dendrites in weld made without arc oscillation; (b) finer dendrites in weld made with transverse arc oscillation. (Magnification 200X) [1]

4.6 Dilution analysis results

Chemical analysis of the 31CrV3, both on the base metal and the weld metal of the specimens 50, 51 and 52 with the gap distances of 0(zero), 1 and 1.5 millimeters are given at the table 4.8.

Table 4.8 Chemical compositions of 31CrV3 on the base metal and specimens 50, 51,52

31CrV3	Chemical composition, max wt%										
	%C	%Si	%Mn	%P	%S	%Cr	%Mo	%Ni	%V	%Al	%Cu
Base metal	0.33	0.27	0.50	0.011	0.029	0.55	0.01	0.08	0.09	0.030	0.20
Specimen 50	0.170	0.551	1.00	0.0216	0.0220	0.184	<0.001	0.0794	<0.001	0.0191	0.104
Specimen 51	0.174	0.587	1.03	0.0237	0.0253	0.166	<0.001	0.0786	<0.001	0.0191	0.0990
Specimen 52	0.168	0.607	1.07	0.0240	0.0240	0.154	<0.001	0.0794	<0.001	0.0191	0.0992

In the present study, since the filler metal contains no chromium, amount of dilution is calculated by comparing the chromium content of the base metal with that measured on the surface of the weld metal. (See equation 3). The dilution for specimens 50, 51 and 52 was found to be 33%, 30% and 28% respectively.

$$\%\text{dilution} = 100\% - [100\% \times (Cr_{BM} - Cr_{WM}) / Cr_{BM}] \quad (3)$$

Table 4.9 Hardness values (H_v) of 31 CrV3 at 3.55 kJ/cm.

Specimen no	Gap distance	Hardness Indentations														
		1	2	3	4	5	6	7	8	9	10	11	12	13	14	15
50	0	211	202	209	380	534	537	337	340	325	590	533	403	207	201	204
51	1	218	215	221	415	493	570	292	297	288	582	497	415	221	220	214
52	1.5	222	219	232	480	548	576	290	295	287	568	565	506	228	217	215

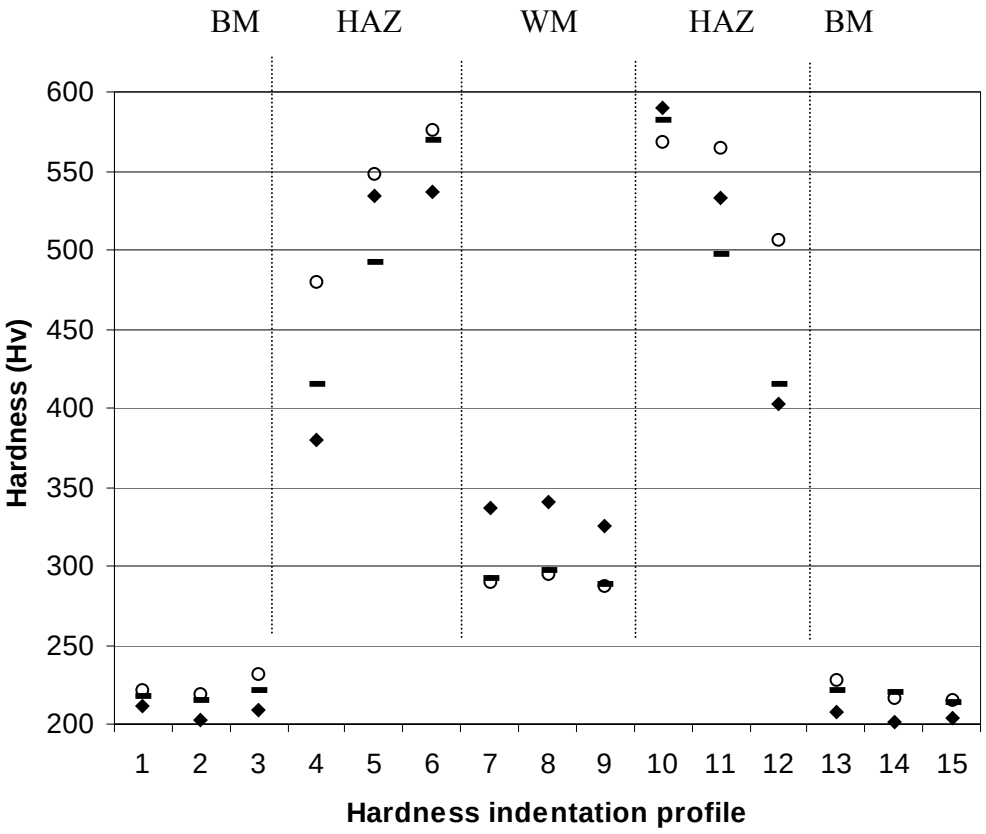

Figure 4.16 Effect of gap distance on hardness, at constant heat input rate.

According to the figure 4.15 there is not any correlation in hardness values with the gap distance in the heat affected zone. However, in the weld metal, particularly considering the o (zero) gap distance hardness indentations, exhibited higher hardness values as expected due to the higher dilution (33%) with respect to the 1 and 1.5 millimeter gap distances (30% and 28% respectively.) The greater amount of chromium in the weld metal increased the hardness value.

The macro-photographs of these three specimens, 50, 51 and 52 with the corresponding gap distances and width of the HAZs are shown at figure 4.15, 4.16 and 4.17, respectively. The width of the HAZ is increasing as the gap distance increase.

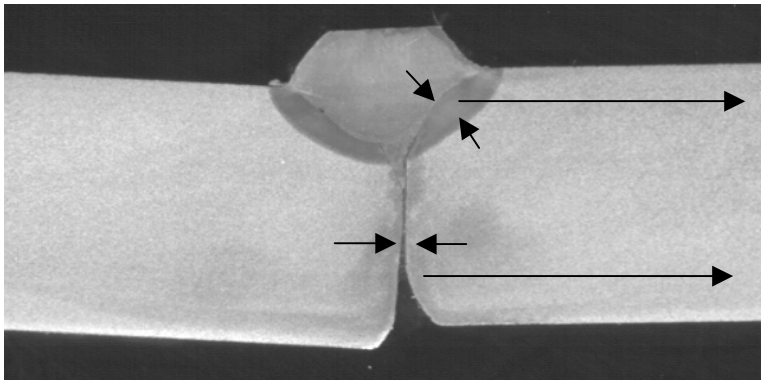

Figure 4.17 Macro-photograph of the specimen 50. (Magnification 5X)

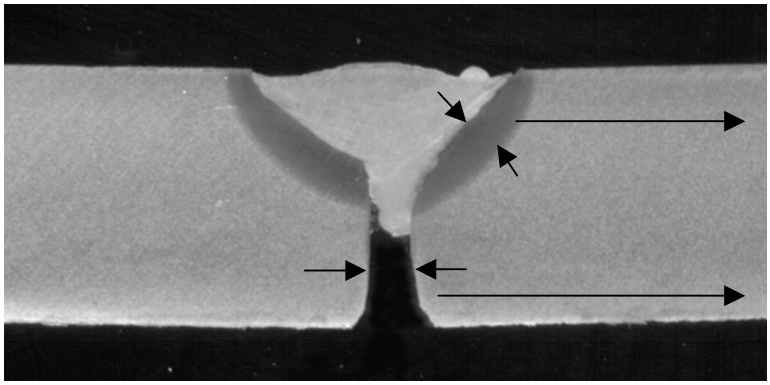

Figure 4.18 Macro-photograph of the specimen 51. (Magnification 5X)

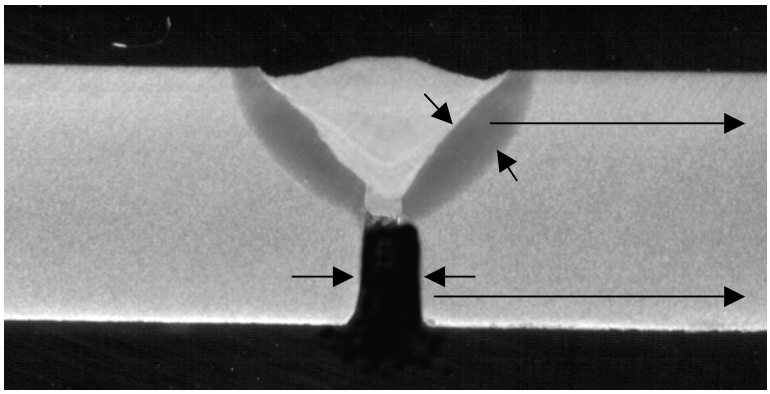

Figure 4.19 Macro-photograph of the specimen 52. (Magnification 5X)

According to Chan et al. [14] “In general, it is assumed that alloying elements in low alloy steels have minimal effect on weld bead geometry”. Therefore, the results of this investigation, an increase in width of HAZ from 1 to 1.4 millimeters can be applied to the increase in gap distance from 0 to 1.5 millimeters.

The higher base metal hardness values of 31CrV3 (ranges from 200 to 230 H_v, figure 4.16) according to the base hardness values of S235 (ranges from100 to 120 H_v, figure 4.2 and 4.6 is due to the higher carbon content of 31CrV3 (0.33 wt%) with respect to S235 (0.22 wt%). However, the drastic increase in the HAZ hardness values of 31CrV3 (ranges from 350 to 600 H_v, figure 4.16), where the HAZ hardness values of S235 (ranges from140 to 180 H_v, figure 4.2 and 4.6), is due to the martensite formation in 31CrV3.

4.7 Tensile test results

Tensile test results of the specimens with the corresponding gap distance, bevel height and heat input values are given at the table 4.10.

Table 4.10 Tensile test results

Specimen No	Ultimate Tensile Strength (MPa)	Elongation %	Gap Distance (mm)	Bevel Height (mm)	Heat Input Rate (kJ/cm)
8	488.9	13.55	0	3	3.18
12	495.5	9.68	1	3	3.18
16	510	8.06	1.5	3	3.18
30	452.5	9.68	1	1	3.55
31	472.3	8.06	1	2	3.55
32	475.4	8.06	1	3	3.55
40	523	14.84	0	3	2.42
44	526.3	11.29	1	3	2.42
48	532	8.06	1.5	3	2.42
Unwelded S235 test coupon	342.8	43.55	-	-	-

Before starting the tensile test, the thickness of the specimens was reduced to 2 mm in order to eliminate the effect of insufficient penetration. By this way, effect of heat input on UTS and % elongation values could be discussed.

Evaluating the ultimate tensile strength and % elongation values given at the table and investigating the fracture surfaces of the specimens, 40, 44 and 48, it is seen that the highest ultimate tensile strength and the maximum % elongation values

obtained. This can be explained by the minimum heat input values, which these specimens exposed to. The same effect can also be said for the specimens 30, 31 and 32, which have the lowest UTS and the minimum % elongation values. The heat input of 3.55 kJ/cm is the maximum heat input used during the experiments, which these specimens exposed to.Similarly, specimens 8, 12 and 16 having heat input of 3.18 kJ/cm have the intermediate UTS and % elongation values among the other set of specimens.

Further discussion can be done on the gap distances of the specimens. Specimens 8 and 40 have the gap distance of 0 mm. For this reason, the amount of dilution is maximum at this gap distance, which was observed in the dilution analysis result of 31CRV3, section 4.6. Similarly, specimens 12 and 44 have lesser dilution and specimens 16 and 48 have the least amount of dilution. i.e the highest amount of filler metal in the weld zone and the least amount of base metal in the weld zone. This caused the highest UTS, however the minimum % elongation which is logical when the UTS and % elongation of the weld metal welded with the G42 G3Si1 and S235 compared. Table 4.11 tabulates the mechanical properties of the weld metal according to EN 440 and unwelded S235 test coupon.

Table 4.11 Mechanical properties of the weld metal and S235

	Ultimate tensile strength MPa	Elongation %
Weld metal	500 – 640	20*
Unwelded S235 test coupon	342.8	43.55

* elongation is the minimum value for the weld metal determined in accordance with the welding conditions specified in EN 440 clause 5.

Similar results observed when the bevel heights were considered. As the bevel height increased from 1 to 3 millimeters, amount of dilution decreased and higher UTS and lower % elongation values obtained.

CHAPTER 5

CONCLUSION

This study was undertaken with the objective of determining the effects of gap distance, bevel height and heat input rate on the mechanical properties and cross sectional characteristics of the MIG/MAG butt welds. With this objective several plates were welded and an experimental study was conducted to investigate these welding parameters. When the whole data obtained from the study are evaluated within the results of the experiments, a consequence for welding parameters is achieved as follows:

(1) The depth of penetration of the weld bead is of high importance because it has a direct influence on weld strength. An increase in voltage preserving short circuiting transfer mechanism (voltage range of 14 to 22 volts), at constant electrode feed rate and constant travel speed, results in an increase in the heat input and hence, increases in the depth of bead penetration in the single pass weldments. However, the voltage values over 19 volts result in spatter and undercut defects,

(2) In the range of 2.42 kJ/cm to 3.55 kJ/cm heat input rate, no significant hardness changes occured in the weld metal. However, in the heat affected zone, hardness increased with decreasing heat input rate,

(3) Gap distance and bevel height are the main geometrical parameters of the weld joint. They affect the amount of dilution, which changes the weld metal composition. Hence, determines the final mechanical properties of the weldment.

REFERENCES

[1] Sindo Kou, “Welding Metallurgy”, second edition, John Wiley & Sons, Inc ,2003

[2] "Welding processes", Welding Handbook, Eight Edition, Volume 2, American Welding Society. 1991. Chap.4

[3] ASM Handbook Volume 6, “Welding, Brazing and Soldering”, 1993

[4] R.D. Stout, “Weldability of Steels”, Welding Research Council, 1987, p. 3–4, 263.

[5] “Metals and Their Weldability”, Welding Handbook, Vol.4, American Welding Society, 1960, p. 61.10

[6] Andrew Daniel Althouse, Carl H. Turnquist, William A. Bowditch, “Modern Welding”, Goodheart-Willcox Co, January 2000, p.53

[7] DIN EN 440, “Wire electrodes and deposits for gas-shielded arc welding of non-alloy and fine-grain steels”, November 1994

[8] DIN EN 439, “Shielding gases for arc welding and cutting”, May 1995

.

[9] DIN EN 1043-1, “Hardness test on arc welded joints” , May 1995

[10] DIN EN 895, “Destructive tests on welds in metallic materials-Transverse tensile test”, June 1995

[11] Dr Sun Zheng, Dr Kuo Min, Pan Dayou, “Twin wire Gas Tungsten Arc Cladding”, SIMTech Technical Report (PT/99/004/JT), Joining Technology Group, Process Technology Division,1999

[12] The Welding Institute, TWI, World Centre for Materials Joining Technology, JoinIT, www.twi.co.uk,

[13] I.S Kim, K.J. Son, Y.S Yang, P.K.D.V Yaragada “Sensitivity analysis for process parameters in GMA welding processes using a factorial design method” International Journal of Machine Tools & Manufacture Vol. 43, 2003

[14] B. Chan, J. Pacey, M. Bibby, “Modelling gas metal arc weld geometry using artificial neural network technology”, Canadian Metallurgical Quarterly, Vol. 38, 1999

[15] V. Gunaraj, N. Murugan, “Prediction and comparison of the heat-affected zone for th bead-on-plate and bead-on-joint in submerged arc welding of pipes.”, Journal of Materials Processing Technology Vol.95, 1999

[16] I.S Kim, J.S Son, I.G Kim, J.Y Kim, O.S Kim, “A study on relationship between process variables and bead penetration for robotic CO_2 arc welding”, Journal of Materials Processing Technology Vol.136, 2003

[17] F. Raoufi, “Parameter optimization in MIG/MAG welding processes”, M.Sc. Thesis, METU, 1994.